Order Number 1335806

# Effects of spacial variation of the thermal coefficient of expansion on optical surfaces

Archer, Robert Joseph, M.S.

The University of Arizona, 1988

# EFFECTS OF SPACIAL VARIATION OF THE THERMAL COEFFICIENT OF EXPANSION ON OPTICAL SURFACES

by

Robert Joseph Archer

---

A Thesis Submitted to the Faculty of the

DEPARTMENT OF CIVIL ENGINEERING AND ENGINEERING MECHANICS

In Partial Fulfillment of the Requirements
For the Degree of

MASTER OF SCIENCE
WITH A MAJOR IN ENGINEERING MECHANICS

In the Graduate College

THE UNIVERSITY OF ARIZONA

1988

## STATEMENT BY AUTHOR

This thesis has been submitted in partial fulfillment of requirements for an advanced degree at the University of Arizona and is deposited in the University Library to be made available to borrowers under rules of the Library.

Brief quotations from this thesis are allowable without special permission, provided that accurate acknowledgment of source is made. Requests for permission for extended quotation from or reproduction of this manuscript in whole or in part may be granted by the head of the major department or the Dean of the Graduate College when in his or her judgment the proposed use of the material is in the interests of scholarship. In all other instances, however, permission must be obtained from the author.

SIGNED: Robert Joseph Anderson

## APPROVAL BY THE THESIS DIRECTOR

This thesis has been approved on the date shown below:

Ralph M. Richard
Professor of Civil Engineering
and Engineering Mechanics

22 Nov 88
Date

## ACKNOWLEDGMENTS

I am grateful to the staff and faculty of the Engineering Mechanics Department for all their assistance. In particular, I would like to thank my advisor, Professor Ralph Richard.

I would also like to thank Dan Vukobratovich of the Optical Sciences Department for his help and guidance.

Most importantly, I would like to thank my wife, Kim, and my sons, Zachary and Corey, for their love and tolerance in spite of long periods of neglect.

TABLE OF CONTENTS

TABLE OF CONTENTS--Continued

# LIST OF ILLUSTRATIONS

LIST OF ILLUSTRATIONS--Continued

# LIST OF TABLES

## ABSTRACT

The deformation of a mirror's optical surface due to a spacial variation of the coefficient of thermal expansion is examined. Four types of variations of the coefficient of thermal expansion are studied. These represent variations which result after typical manufacturing and/or fabrication processes.

Equations describing the deformations resulting from the variations in the coefficient of thermal expansion are derived for some of the cases. Deformations due to more complex variations in the coefficient of thermal expansion are developed empirically using data generated by the finite-element method.

# Chapter 1

## INTRODUCTION

An important factor in the design of metal optical mirrors is the prediction of deformations due to thermal loads. Metals have a much larger thermal expansion coefficient than the commonly used optical materials. This relatively large thermal expansion coefficient can be the source of deformations that are large enough to adversely affect optical performance.

The subject of this thesis is the effect that small variations in the thermal expansion coefficient through the mirror body have on mirrors undergoing a temperature change. In this case the mirror is figured at some temperature and then is brought to thermal equilibrium at a new temperature. The variation in the thermal expansion coefficient will cause the mirror to expand or contract different amounts at different locations which causes the optical surface to deform.

There are four types of variations of the thermal expansion coefficient discussed in this thesis. The first is a linear variation of the thermal expansion coefficient along any or all of the axes of a Cartesian coordinate system with one axis parallel to the optical axis. The second is any variation through the thickness of the mirror; a quadratic variation is described in more detail. The third function is a linear variation in the plane of the mirror which increases or

decreases radially from the center of the mirror. The fourth function is a linear variation in the plane of the mirror which increases or decreases radially from some point that is not at the center of the mirror.

These four functions were chosen because they represent variations in the thermal expansion coefficient which have been measured following the manufacture of the mirror blank.

The remainder of the thesis is divided into six chapters. In the first of these chapters, the coordinate systems, the unit system, and the four functions which define the variations in the thermal expansion coefficient are defined.

The deformations caused by the four functions of the thermal expansion coefficient are described in the next four chapters. Each of these chapters is divided into two parts: (1) the derivation of a function which describes the deformations, and (2) a comparison of the derived function with the results of a finite-element model.

The final section contains suggestions for future work to be undertaken in this study.

There are two appendices included at the end of this thesis. Appendix A contains a program which was used to develop the input file for the NASTRAN finite-element program, and the instructions for using the program. Appendix B contains tables of the optical aberrations that were produced by specific cases of the four functions of the thermal expansion coefficient.

# Chapter 2

# DEFINITIONS

In this section, the coordinate systems, symbols, and conventions used throughout the remainder of the report are discussed.

## Units

In order to make the equations easier to apply, the unit of length will be the mirror radius. For example, a mirror with a 6:1 diameter-to-thickness ratio has a thickness of 1/3 mirror radii. The coefficient of thermal expansion is in units of length over length per degree Kelvin.

## Defining the Mirror

The mirrors that are modeled in this report are cylindrical with a flat bottom. The distance from the center of the bottom to the center of the top is $h$ mirror radii. For a flat mirror, $h$ is the thickness throughout the mirror.

The distance $h$ is related to the diameter-to-thickness ratio, $D/t$, as shown in Equation 2-1.

$$h = \frac{2}{D/t} \tag{2-1}$$

The axial radius, $\rho$, defines the curvature of the optical surface and is shown in Figure 2-1. The diameter-to-thickness ratio and the axial radius completely define the geometry of the mirror.

Coordinate Systems

Two coordinate systems are used in this report: (1) a Cartesian coordinate system, and (2) a cylindrical coordinate system. The origin of both coordinate systems is located at the center of the bottom of the mirror.

The Cartesian coordinate system is right-handed and is oriented so that the $z$ axis is up, and the $x$ and $y$ axes are in the plane of the bottom of the mirror (see Figure 2-2).

The $z$ axis of the cylindrical coordinate system is coincident with the $z$ axis defined above. The $r$ and $\theta$ axes are in the plane of the bottom of the mirror. The angle $\theta$ is measured from the x axis using the right-hand rule.

Coefficient of Thermal Expansion

The coefficient of thermal expansion is a function of position in the mirror. For this report, the following four classes of variations will be considered:

1. Linear variation along the coordinate axes.
2. Quadratic variation along the $z$ axis.
3. Linear variation in the radial direction.
4. Linear variation along the radial direction of a coordinate system which is offset from the center of the mirror.

Case 1. For a linear variation along the Cartesian axes, the distribution of the coefficient of thermal expansion ($\alpha$) is described

by three percentages $p_x$, $p_y$, and $p_z$, where

$p_x$ = the percent change in $\alpha$ from $x = 0$ to $x = 1$

$p_y$ = the percent change in $\alpha$ from $y = 0$ to $y = 1$

$p_z$ = the percent change in $\alpha$ from $z = 0$ to $x = h$

The equation describing the distribution of $\alpha$ is

$$\alpha_1(x,y,z) = \alpha_0\left(1 + p_x x + p_y y + \frac{p_z z}{h}\right) \tag{2-2}$$

Case 2. For the quadratic variation along the $z$ axis, one value, $p_q$, describes the distribution of $\alpha$ throughout the mirror. Where $p_q$ is the percent change from the bottom of the mirror to the top. Equation 2-3 is $\alpha$ as a function of $z$.

$$\alpha_2(z) = \alpha_0\left(1 + \frac{p_q z^2}{h^2}\right) \tag{2-3}$$

Case 3. The third case is a linear variation of $\alpha$ in the radial direction. The function $\alpha$ is only a function of the coordinate $r$ and is defined by the parameter $p_r$, which is the percent change in $\alpha$ from the center of the mirror to the outside edge of the mirror cylinder.

$$\alpha_3(r) = \alpha_0(1 + p_r r) \tag{2-4}$$

Case 4. The $\alpha$ distribution for case 4 is shown in Figure 2-3. The distance $\delta$ is the distance from the origin of a radial distribution

of $\alpha$ to the center of the mirror. Both origins are in the $x$-$y$ plane. The parameter $p_\delta$ is the percent change in $\alpha$ from the mirror center to the point $x = 1$, $y = 0$.

$$\alpha_4(x,y) = \alpha_0\{1 + p_\delta[(x + \delta)^2 + y^2\ ]^{1/2} - \delta\} \qquad (2\text{-}5)$$

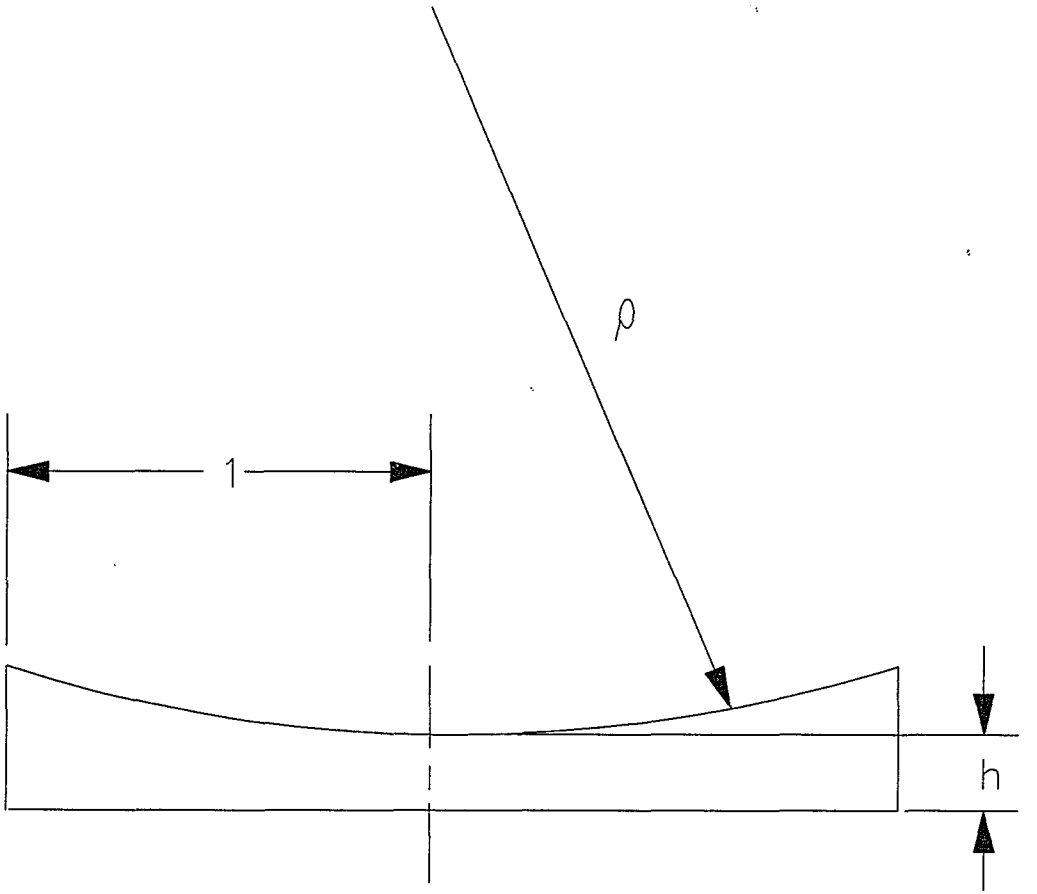


Figure 2–1
Mirror Shape Parameters

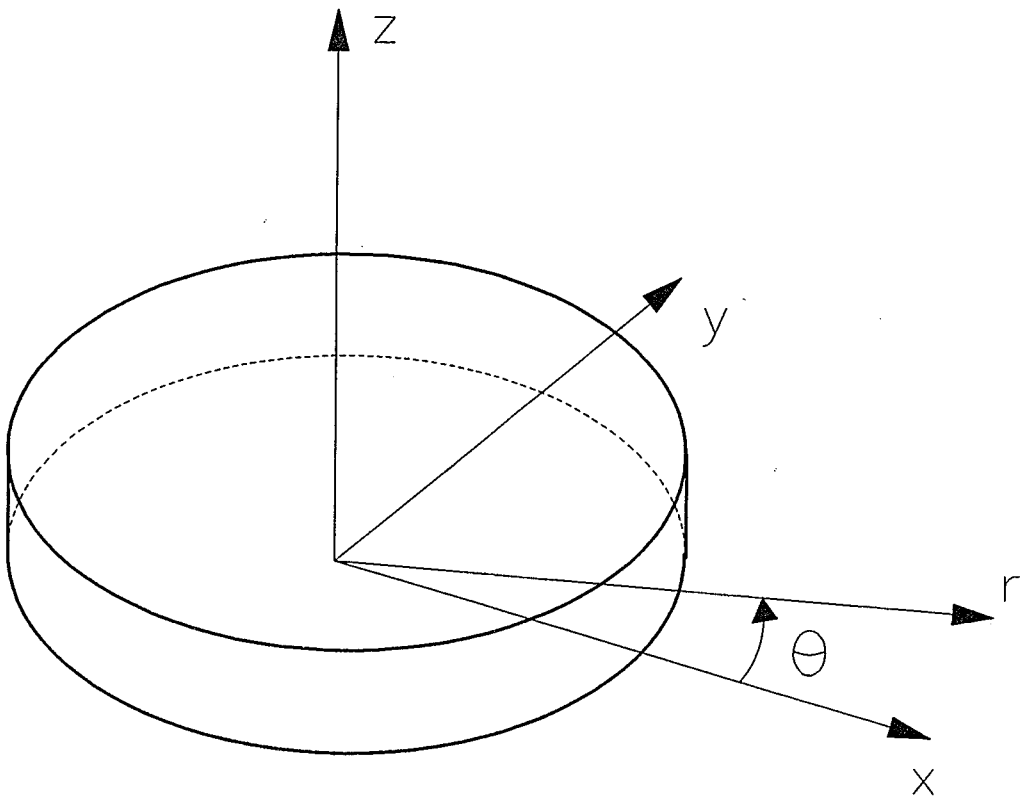


Figure 2–2
Coordinate Systems

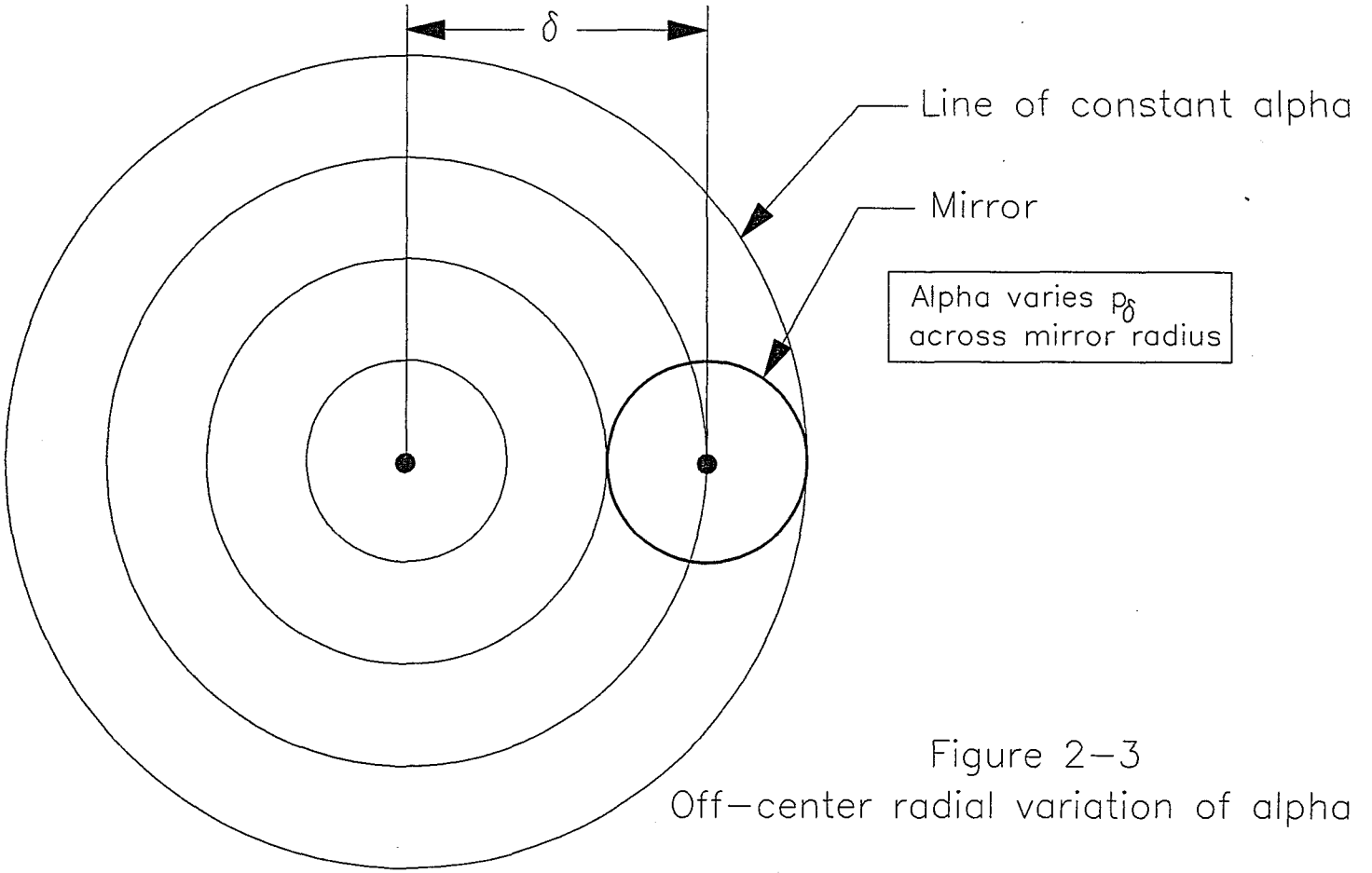


Figure 2–3
Off–center radial variation of alpha

# Chapter 3

## CASE 1: LINEAR VARIATION ALONG THE COORDINATE AXES

The displacements caused by a linear variation in the thermal expansion coefficient along the Cartesian coordinate axes are described in this chapter. The first section is a derivation of the displacement equations. The second section contains the results of a comparison between the theoretically derived model and a finite-element model using NASTRAN.

### Derivation

From chapter 2, the distribution of $\alpha$ for case 1 can be written

$$\alpha(x,y,z) = \alpha_o\left(1 + p_x x + p_y y + \frac{p_z z}{h}\right) \qquad (3\text{-}1)$$

It is easier to work with the product $T\alpha(x,y,z)$, where $T$ is the change in temperature from when the mirror was figured. For clarity, $k$ is used to represent the product $\alpha(x,y,z)T$ so that

$$k(x,y,z) = k_0 + k_x x + k_y y + k_z z \qquad (3\text{-}2)$$

Where: $k_0 = \alpha_0 T$

$k_x = p_x \alpha_0 T$

$k_y = p_y \alpha_0 T$

$k_z = \frac{p_z \alpha_0}{h} T$

The stress-strain relations, including the terms for thermal expansion are

$$\varepsilon_x = \frac{1}{E}\left[\sigma_x - \mu(\sigma_y + \sigma_z)\right] + \alpha T$$

$$\varepsilon_y = \frac{1}{E}\left[\sigma_y - \mu(\sigma_x + \sigma_z)\right] + \alpha T$$

$$\varepsilon_z = \frac{1}{E}\left[\sigma_z - \mu(\sigma_x + \sigma_y)\right] + \alpha T \qquad (3\text{-}3)$$

$$\varepsilon_{xy} = \frac{1}{2G}\sigma_{xy}$$

$$\varepsilon_{yz} = \frac{1}{2G}\sigma_{yz}$$

$$\varepsilon_{zx} = \frac{1}{2G}\sigma_{zx}$$

Where: $\varepsilon$ = strain

$\sigma$ = stress

$E$ = Modulus of Elasticity

$\mu$ = Poisson's Ratio

$G = \frac{E}{2(1+\mu)}$

Assuming that there is no stress developed from the thermal

strains, all the stress terms drop out and Equations 3-3 become

$$\begin{aligned} \varepsilon_x &= k_0 + k_x x + k_y y + k_z z \\ \varepsilon_y &= k_0 + k_x x + k_y y + k_z z \\ \varepsilon_z &= k_0 + k_x x + k_y y + k_z z \\ \varepsilon_{xy} &= \varepsilon_{yz} = \varepsilon_{zx} = 0 \end{aligned} \tag{3-4}$$

The strain displacement relations are

$$\begin{aligned} \varepsilon_x &= \frac{\partial u}{\partial x} \\ \varepsilon_y &= \frac{\partial v}{\partial y} \\ \varepsilon_z &= \frac{\partial w}{\partial z} \\ \varepsilon_{xy} &= \frac{1}{2}\left(\frac{\partial u}{\partial y} + \frac{\partial v}{\partial x}\right) \\ \varepsilon_{yz} &= \frac{1}{2}\left(\frac{\partial v}{\partial z} + \frac{\partial w}{\partial y}\right) \\ \varepsilon_{zx} &= \frac{1}{2}\left(\frac{\partial w}{\partial x} + \frac{\partial u}{\partial z}\right) \end{aligned} \tag{3-5}$$

Substituting Equation 3-4 into Equation 3-5 for the normal strains

results in

$$\frac{\partial u}{\partial x} = \frac{\partial v}{\partial y} = \frac{\partial w}{\partial z} = k_0 + k_x x + k_y y + k_z z \tag{3-6}$$

Integrating Equations 3-6 yields

$$\begin{aligned} u &= \frac{k_x x^2}{2} + x(k_y y + k_z z + k_0) + f(y,z) \\ v &= \frac{k_y y^2}{2} + y(k_x x + k_z z + k_0) + g(x,z) \\ w &= \frac{k_z z^2}{2} + z(k_x x + k_y y + k_0) + h(x,y) \end{aligned} \tag{3-7}$$

The functions $f$, $g$, and $h$ are unknown functions from the integration. They can be found by applying the boundary conditions and the shear strain conditions. Assume the following forms for $f$, $g$, and $h$.

$$\begin{aligned} f(y,z) &= -\tfrac{1}{2} k_x y^2 - \tfrac{1}{2} k_x z^2 + a_1 y + b_1 z + c_1 \\ g(x,z) &= -\tfrac{1}{2} k_y x^2 - \tfrac{1}{2} k_y z^2 + a_2 x + b_2 z + c_2 \\ h(x,y) &= -\tfrac{1}{2} k_z x^2 - \tfrac{1}{2} k_z y^2 + a_3 x + b_3 y + c_3 \end{aligned} \tag{3-8}$$

Combining Equations 3-7 and 3-8, and substituting them into

Equations 3-5 for the shear strains produces

$$\frac{\partial u}{\partial y} + \frac{\partial v}{\partial x} = 0 = k_y x - k_x y + a_1 + k_x y - k_y x + a_2$$

$$\frac{\partial v}{\partial z} + \frac{\partial w}{\partial y} = 0 = k_z y - k_y z + b_2 + k_y z - k_z y + b_3 \qquad (3\text{-}9)$$

$$\frac{\partial w}{\partial x} + \frac{\partial u}{\partial z} = 0 = k_x z - k_z x + a_3 + k_z x - k_x z + b_1$$

Solving Equation 3-9 for $a_2$, $b_3$, and $b_1$ results in

$$a_2 = -a_1$$

$$b_3 = -b_2 \qquad (3\text{-}10)$$

$$b_1 = -a_3$$

The total displacements are shown in Equation 3-11.

$$u = \frac{1}{2} k_x x^2 - \frac{1}{2} k_x (y^2 + z^2) + x(k_y y + k_z z + k_0) + a_1 y - a_3 z + c_1$$

$$v = \frac{1}{2} k_y y^2 - \frac{1}{2} k_y (x^2 + z^2) + y(k_x x + k_z z + k_0) + b_2 z - a_1 x + c_2 \qquad (3\text{-}11)$$

$$w = \frac{1}{2} k_z z^2 - \frac{1}{2} k_z (x^2 + y^2) + z(k_x x + k_y y + k_0) + a_3 x - b_2 y + c_3$$

The constants $a_1$, $b_1$, and $a_3$ represent rigid body rotations. The constants $c_1$, $c_2$, and $c_3$ represent rigid body displacements. These constants can be found by applying the boundary conditions.

Comparison with a Finite-Element Solution

To check the accuracy of the theoretical model, some sample models

were solved using the theoretical solution and a NASTRAN finite-element solution.

The Finite-Element Model. The mirrors were modeled using the NASTRAN finite-element program. The models were made up of the PENTA and HEXA elements as shown in Figure 3-1. The PENTA element is a five-sided, solid, pie-shaped element with from six to fifteen nodes. The HEXA element is a six-sided, solid, brick element with from eight to twenty nodes. For these tests, the six-noded PENTA and the eight-noded HEXA were used.

The elements were arranged in a radial pattern (see Figure 3-1), and the layers of elements were stacked to provide the desired thickness. The total number of elements in a model was varied by changing the number of elements from the center to the outside edge and the number of layers of elements. The number of elements around the circumference was three times the number of elements from the center to the outside edge.

Mathematically, the product of $\alpha(x,y,z)T$ can be made equal to some function $\alpha_0 T(x,y,z)$. Therefore, the numerical models used a variation in nodal temperature to represent the variation in the thermal expansion coefficient instead of assigning a value for $\alpha$ to each element. This has two advantages: (1) it is possible to set up multiple temperature loading cases using one stiffness matrix, and (2) assigning temperature to the nodes instead of assigning $\alpha$'s to the elements allows a finer discretization of $\alpha$-distribution.

The NASTRAN models were constrained so that the center of the

mirror surface could not move in any direction and the bottom center could only move along the $z$ axis. Also, the mirror was constrained at the edge so that it would not rotate about the $z$ axis.

A program was written to generate a NASTRAN input file for the various cases studied in this report. The FORTRAN source code for this program is included in Appendix A along with the instructions for its use.

Boundary Conditions. To compare the theoretical model with the NASTRAN model the values for the unknown constants in Equation 3-11 were needed so that the boundary conditions would match.

Along the $z$ axis there is no displacement in the $x$ and $y$ directions. Substituting these values into Equations 3-11 results in

$$c_1 = c_2 = 0 \tag{3-12}$$

At the center of the mirror surface there is no displacement in any direction. Substituting this information into Equations 3-11 produces

$$\begin{aligned} u(0,0,h) &= 0 = -\tfrac{1}{2} k_x h^2 - a_3 h \\ v(0,0,h) &= 0 = -\tfrac{1}{2} k_y h^2 + b_2 h \\ w(0,0,h) &= 0 = \tfrac{1}{2} k_z h^2 + k_0 h + c_3 \end{aligned} \tag{3-13}$$

Solving Equation 3-13 for the unknown constants yields

$$a_3 = -\frac{1}{2} k_x h$$

$$b_2 = -\frac{1}{2} k_y h \qquad (3\text{-}14)$$

$$c_3 = -\frac{1}{2} k_3 h^2 + k_0 h$$

To prevent rotation around the $z$ axis, $a_1$ is zero.

Since most of the optical effects occur from displacements in the $z$ direction, only the $w$ equation will be examined. After substituting the constants from the boundary conditions, Equation 3-11 becomes

$$w = \frac{1}{2} k_z z^2 - \frac{1}{2} k_z (x^2 + y^2) + z(k_x x + k_y y + k_0)$$
$$- \frac{1}{2} k_y hy - \frac{1}{2} k_x hx - \frac{1}{2} k_z h^2 - k_0 h \qquad (3\text{-}15)$$

Defining the Mirror Surface. Deformations occur throughout the mirror, but the deformation of the top surface is what affects the optics. For a flat mirror, the top surface is the $z = h$ surface. For a mirror with a spherical surface, the surface is a function of the distance along the cylindrical coordinate, $r$.

Let $\rho$ be the radius of curvature of the top surface of the mirror as shown in Figure 3-2. The surface of the mirror as a function of $\rho$ is

$$z = h + \rho(1 - \cos\phi) \qquad (3\text{-}16)$$

Using the Taylor's series expansion for the cosine, Equation 3-16 can be rewritten as

$$z = h + \rho(1 - 1 + \frac{\phi^2}{2} + \textit{higher order terms}) \tag{3-17}$$

And since $\phi$ is approximately equal to $r/\rho$, Equation 3-17 becomes

$$z \cong h + \frac{r^2}{2\rho} \tag{3-18}$$

Substituting Equation 3-18 into Equation 3-15 yields

$$w = \frac{1}{2} k_z \left( \frac{hr^2}{\rho} + \frac{r^4}{4\rho^2} - r^2 \right) + (k_x x + k_y y + k_0) \left( h + \frac{r^2}{2\rho} \right) - \frac{1}{2} k_x hx - \frac{1}{2} k_y hy - k_0 h \tag{3-19}$$

Results for Case 1. To test the theoretical solution, the analytical solution was compared with a numerical solution for four different test cases. Using NASTRAN, each of the test cases was solved four times, increasing the number of elements each time.

All four tests modeled a mirror with a 6:1 diameter-to-thickness ratio. The coefficient of thermal expansion at the origin ($\alpha_0$) was 23.4 x $10^{-6}/K$, and the temperature change was 1 $K$. The parameter, $p_y$, was zero in all four test cases.

For tests A and B, $p_x$ = 0 and $p_z$ = 5%. The axial radius, $\rho$, was infinity for test A, which implies a flat mirror. For test B, $\rho$ is 20 mirror radii. For tests C and D, $p_x$ = 2.5% and $p_z$ = 3%. Test C is a

flat mirror, and $\rho$ is 20 mirror radii for test D. A summary of these parameters is shown in Table 3-1.

| Table 3-1 | Inputs for Tests A through D | | |
|---|---|---|---|
| | $p_x$ | $p_z$ | $\rho$ |
| Test A | 0% | 5% | $\infty$ |
| Test B | 0% | 5% | 20 radii |
| Test C | 2.5% | 3% | $\infty$ |
| Test D | 2.5% | 3% | 20 radii |

Figure 3-3 is a drawing of the cross-section of a mirror that has undergone displacements caused by a variation of $\alpha$ through the thickness. Figure 3-4 is a cross-section of a mirror with $\alpha$ varying in the $x$ direction.

To simplify the comparison of the theoretical and the numerical models, the displacement of a single point is examined. The point chosen is at $(1,0,h + \frac{1}{2}\rho)$, and it is located at the outside edge of the mirror cylinder and on the surface. This point was chosen because it generally had the largest deviation from the analytical solution.

The results of the four theoretical solutions and the sixteen numerical solutions are shown in Table 3-2. Under each displacement, Table 3-2 also contains the percentage of the analytical solution that the displacement represents.

Figures 3-5 through 3-8 contain graphs of the percentages listed in Table 3-2.

Table 3-2
Results of NASTRAN Models and Theoretical Models

| Test | | Theoretical | NASTRAN | | | |
|---|---|---|---|---|---|---|
| | | | 144 Elements | 300 Elements | 540 Elements | 735 Elements |
| A | Displacement | -1.755 | -1.668 | -1.700 | -1.718 | -1.728 |
| | % of Theoretical | | 95.0 | 96.9 | 97.9 | 98.5 |
| B | Displacement | -1.140 | -1.056 | -1.086 | -1.103 | -1.113 |
| | % of Theoretical | | 92.6 | 95.3 | 96.8 | 97.7 |
| C | Displacement | -.9555 | -.9046 | -.9231 | -.9335 | -.9397 |
| | % of Theoretical | | 94.7 | 96.6 | 97.7 | 98.3 |
| D | Displacement | -.3377 | -.2889 | -.3006 | -.3165 | -.3225 |
| | % of Theoretical | | 85.6 | 90.8 | 93.7 | 95.5 |

Notes:
1. Displacement units are mirror radii times $10^6$
2. Test A -- p3 = 5%, rho = $\infty$
3. Test B -- p3 = 5%, rho = 20
4. Test C -- p1 = 2.5%, p3 = 3%, rho = $\infty$
5. Test D -- p1 = 2.5%, p3 = 3%, rho = 20

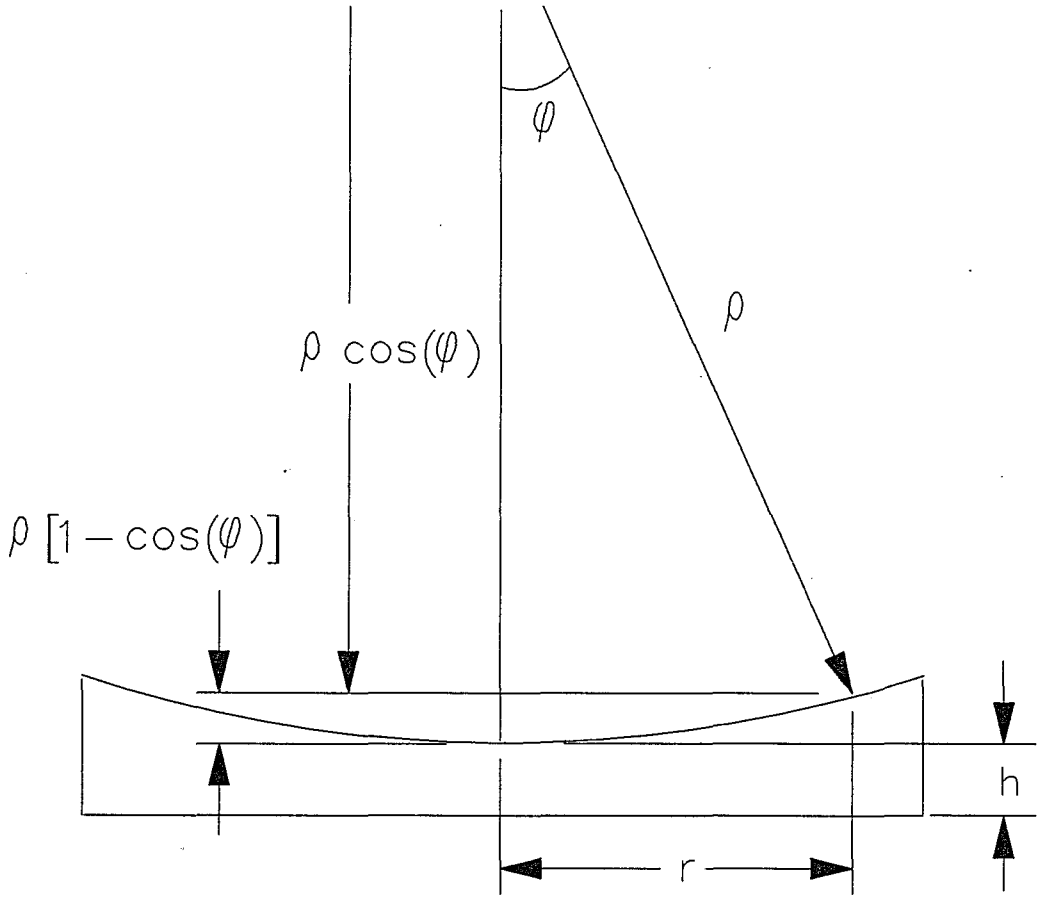


Figure 3–1
The Mirror Surface as a Function of the Curvature

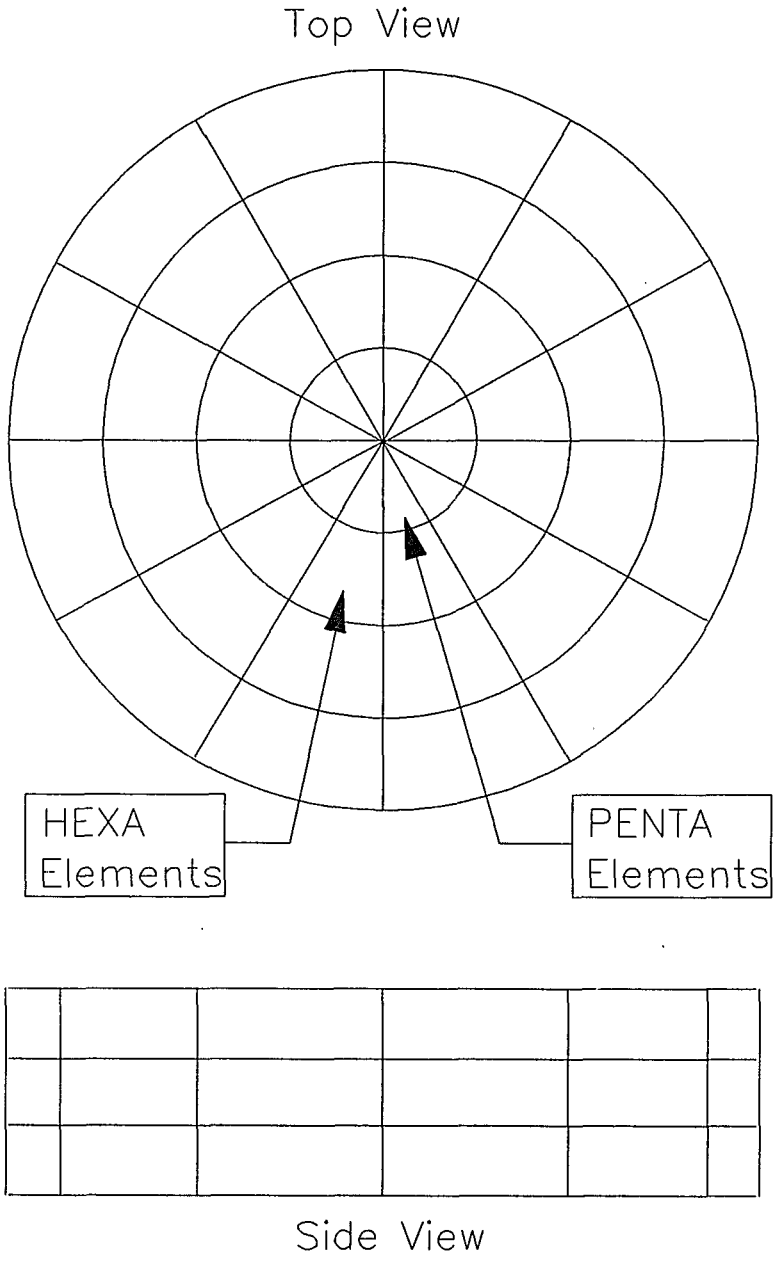


Figure 3–2
NASTRAN Element Layout

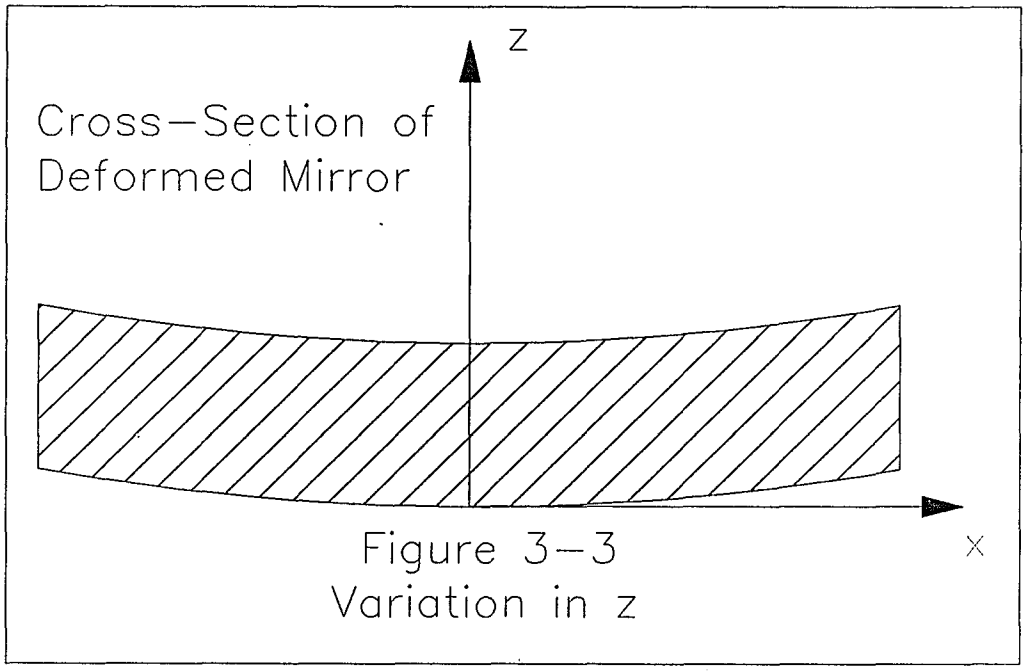


Figure 3–3
Variation in z

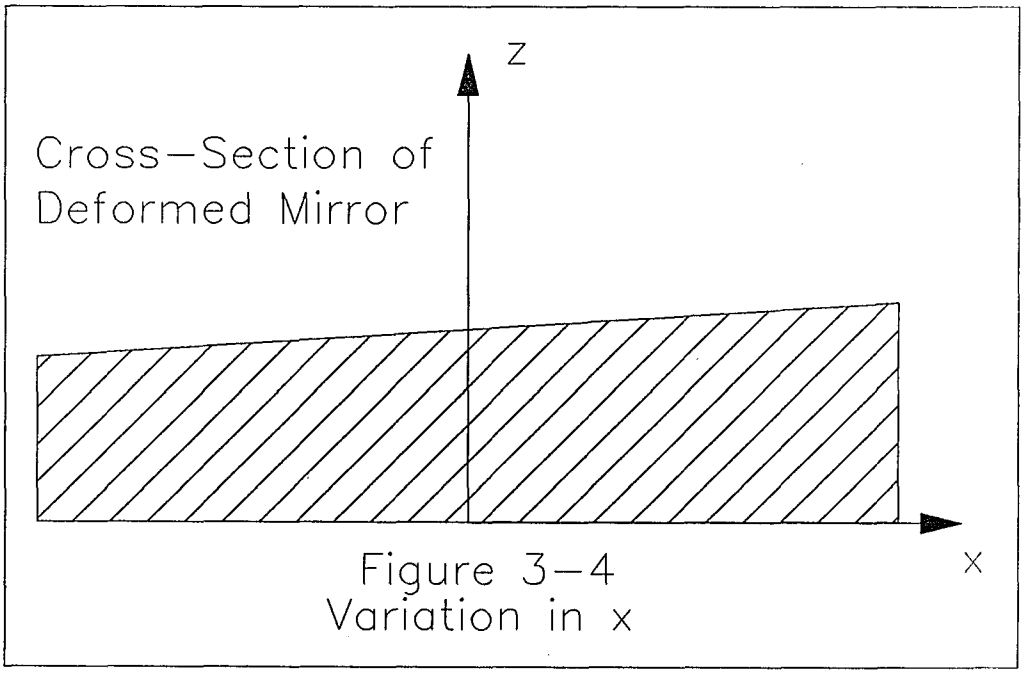


Figure 3–4
Variation in x

# Figure 3-5

Results of Test A

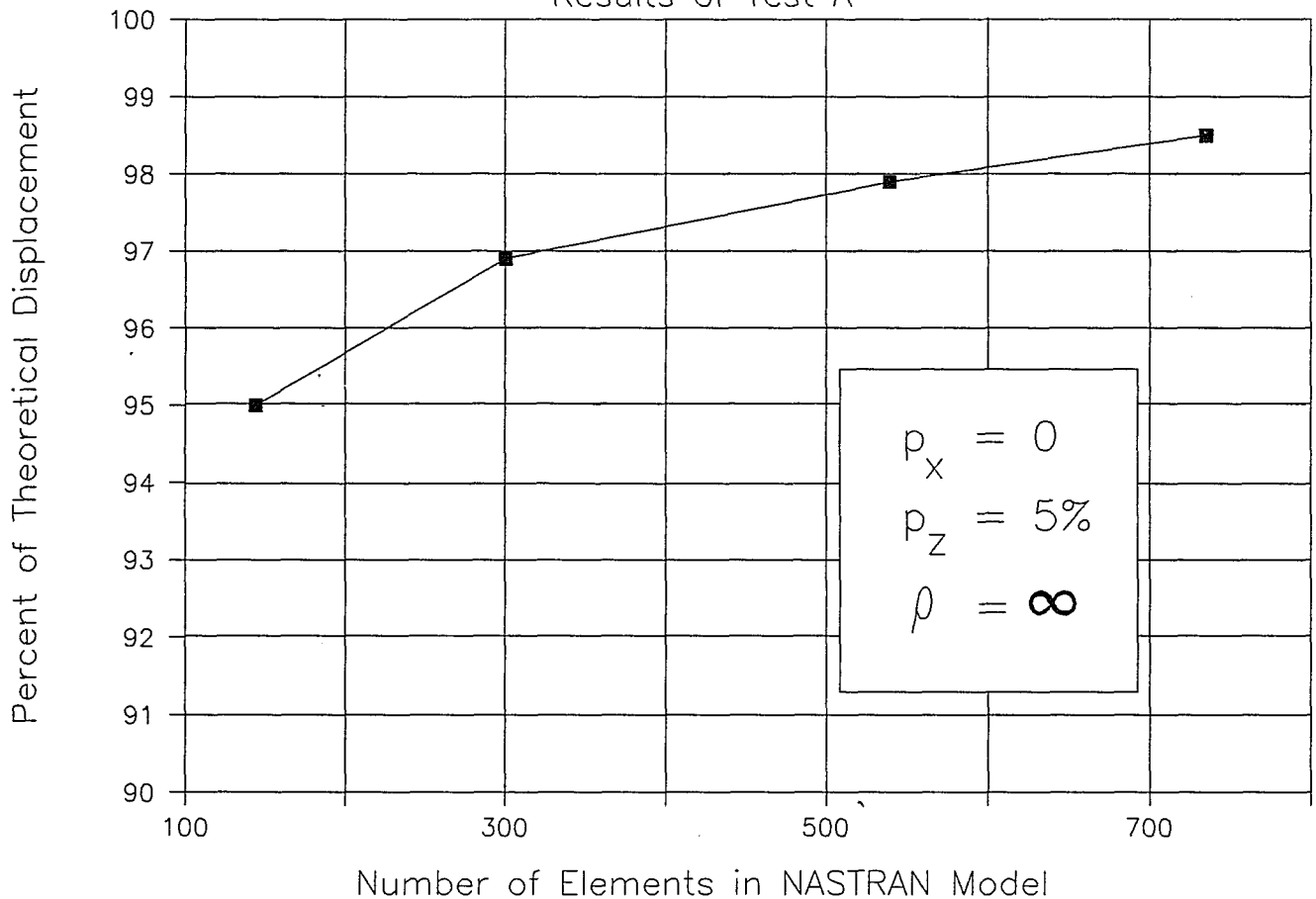

# Figure 3-6

Results of Test B

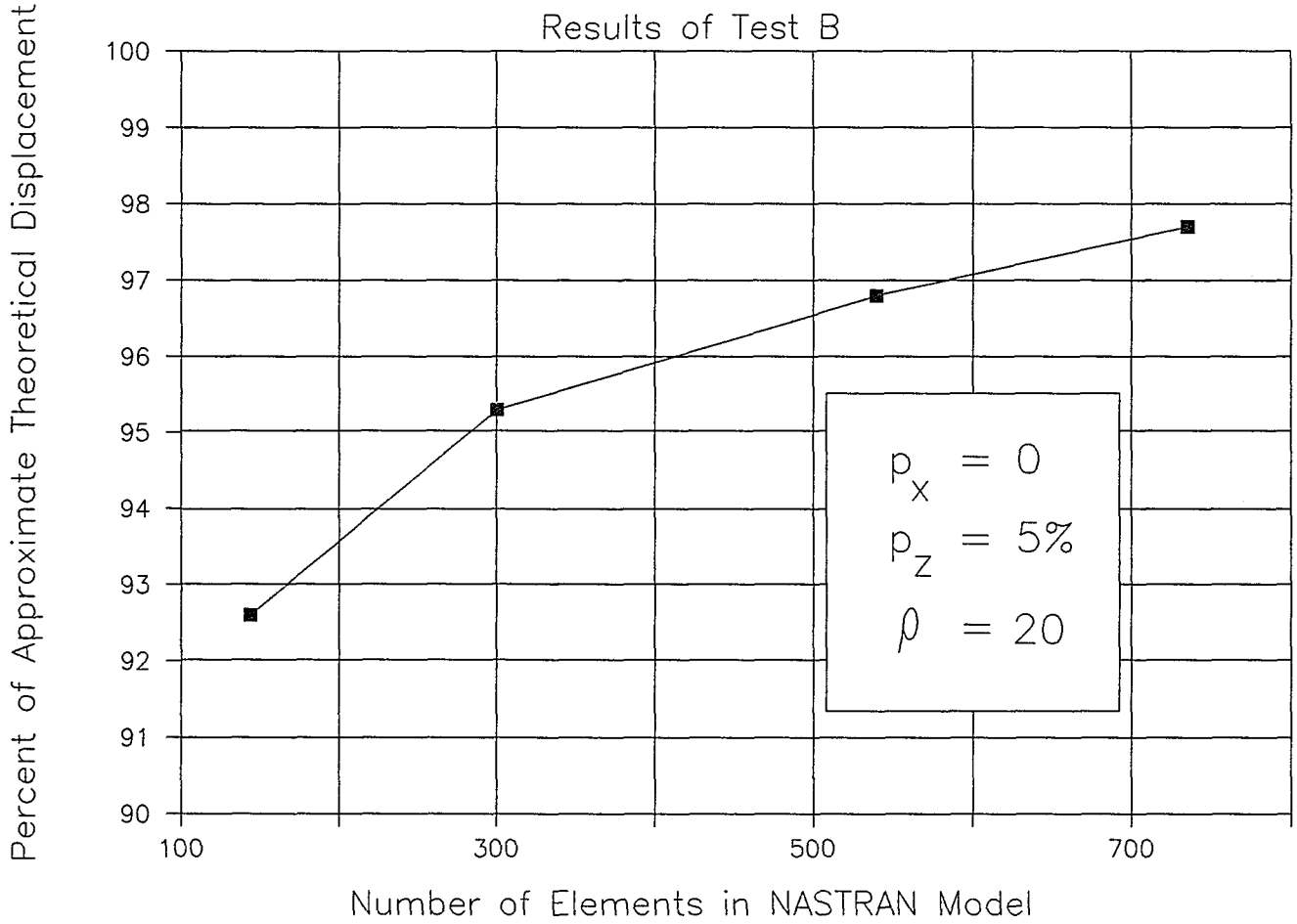

# Figure 3-7

Results of Test C

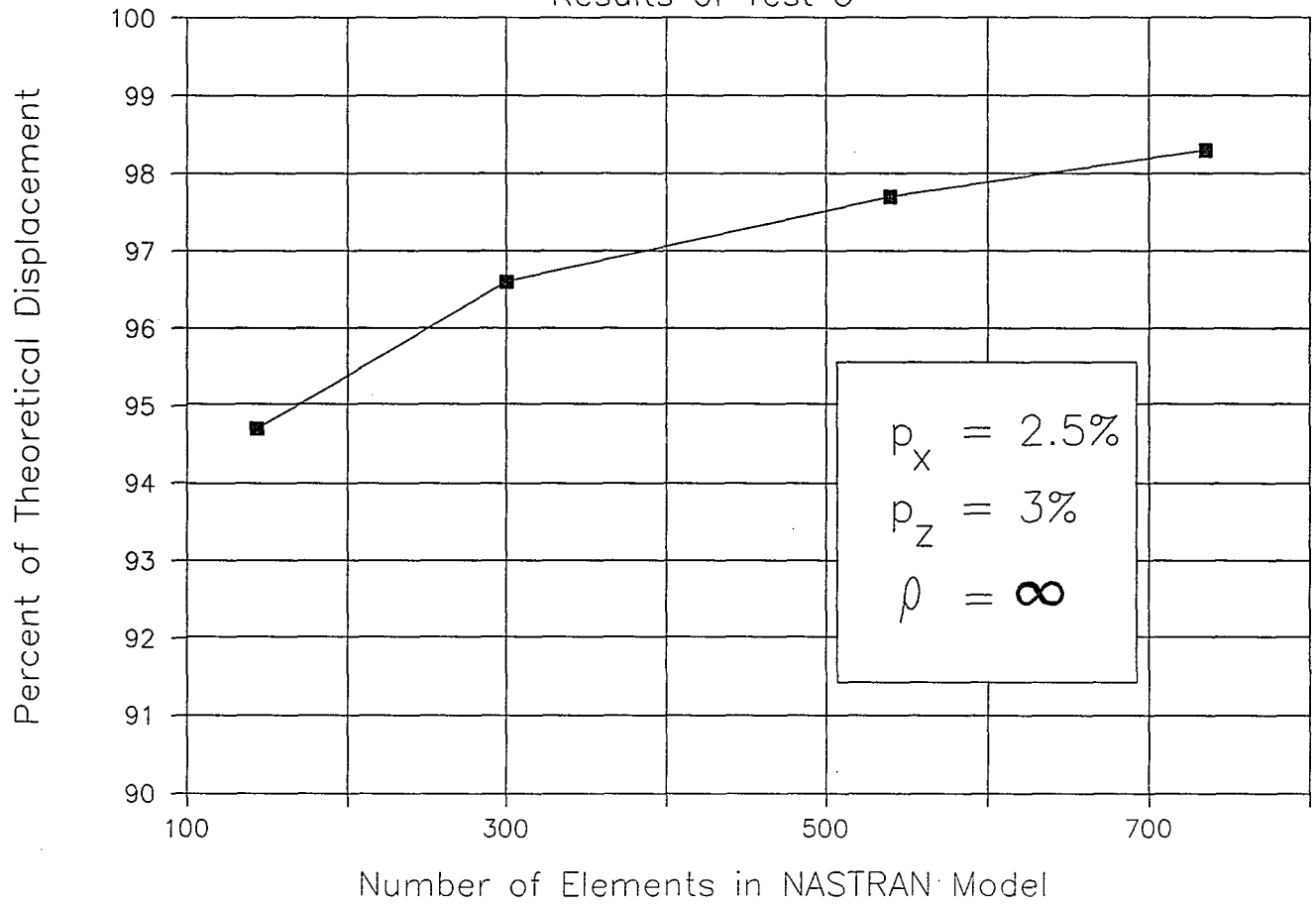

# Figure 3-8

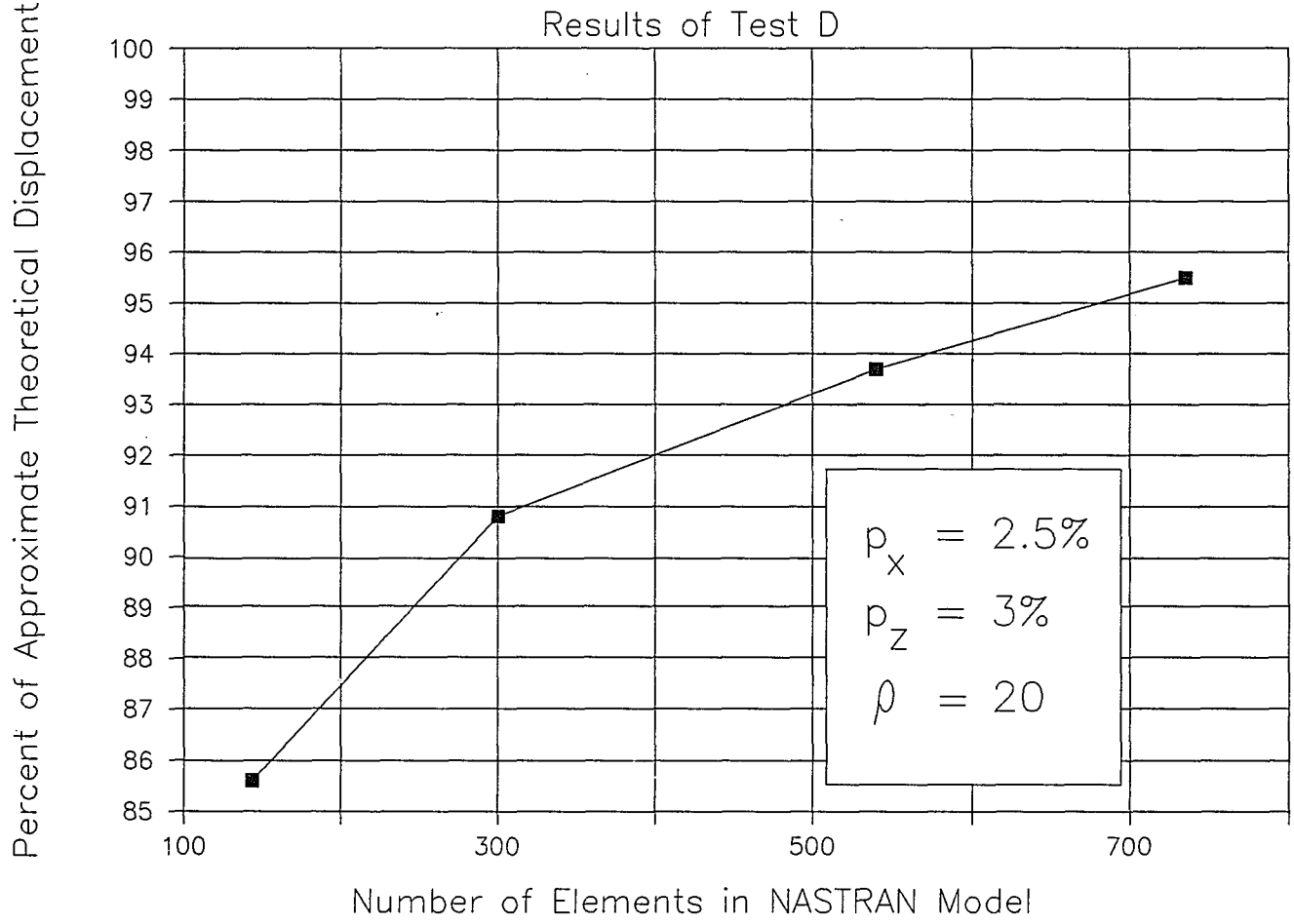
Results of Test D
Percent of Approximate Theoretical Displacement
100
99
98
97
96
95
94
93
92
91
90
89
88
87
86
85
100
300
500
700
Number of Elements in NASTRAN Model
$p_x$ = 2.5%
$p_z$ = 3%
$\rho$ = 20

# Chapter 4

## CASE 2: QUADRATIC VARIATION THROUGH THE THICKNESS

The subject of this chapter is the displacements caused by a variation in the thermal expansion coefficient in the $z$ direction. The chapter is composed of two parts. The first part is a derivation of the $z$ displacement caused by $\alpha(z)$. The second part is a comparison of the theoretical solution with a finite-element solution for a mirror with a quadratic variation of $\alpha$ through the thickness.

### Derivation

To find the displacements, assume that moments are applied to the mirror such that the mirror does not deform due to the combination of thermal strains and the applied moments. Next, apply equal and opposite moments. The net applied moment is zero and the resulting displacements are due to the thermal strains.

The relation between stress, strain, and thermal strain is given in equation 3-3. The applied moment causes the strains to go to zero. Also, due to symmetry $\sigma_x = \sigma_z = \sigma(z)$. If $\sigma_z$ is assumed to be negligibly small, the resulting equation is

$$\sigma(z) = - \frac{\alpha T E}{1-\mu} \tag{4-1}$$

As shown in Figure 5-1, the applied moment is equal to the moment

caused by the stresses at the mirror boundary. The applied moment is

$$M_1 = \int_0^h \sigma(z)\left(z - \frac{h}{2}\right)dz \qquad (4\text{-}2)$$

Now apply an equal but opposite moment to the mirror. According to Timoshenko and Goodier (Reference 1), a square, flat plate with equal moments applied to each side will be bent so that the surface is spherical with a radius of curvature of $R$. The moment as a function of the radius of curvature is

$$M_2 = -M_1 = \frac{Eh^3}{12(1 - \mu)R} \qquad (4\text{-}3)$$

The $z$ displacement caused by the spherical bending of the plate, $w^*$, can be approximated by the relation

$$R = \frac{r^2}{2w^*} \qquad (4\text{-}4)$$

Using superposition, the displacements caused by the two applied moments can be added. Combining Equations 4-1 through 4-4, the resulting displacement is

$$w^* = \frac{-Tr^2 12}{2h^2}\int_0^h \alpha(z)\left(z - \frac{h}{2}\right)dz \qquad (4\text{-}5)$$

However, this is not the total z displacement. The expansion of

the material in the mirror will cause the mirror to grow uniformly in the $z$ direction. This growth is the integrated sum of the expansion of all the elements through the thickness of the mirror. The total $z$ displacement of the mirror is

$$w = \frac{-Tr^2 12}{2h^3}\int_0^h \alpha(z)\left(z - \frac{h}{2}\right)dz + T\int_0^z \alpha(\tau)d\tau + c \qquad (4\text{-}6)$$

where $c$ represents a rigid body displacement which can be found by applying the boundary conditions. In Equation 4-6 it is assumed that there are no rigid body rotations.

Comparison with the Finite-Element Solution

The theoretical model was compared to a finite-element solution for two test problems. Each of the problems modeled a quadratic variation of the thermal expansion coefficient through the thickness.

The NASTRAN models were the same as those in Chapter 3 except that the temperature load represented the quadratic distribution of the thermal expansion coefficient.

Theoretical Solution. The quadratic distribution of the thermal expansion coefficient is

$$\alpha(z) = \alpha_0\left(1 + \frac{p_q}{h^2} z^2\right) \qquad (4\text{-}7)$$

Substituting this distribution into Equation 4-6 results in

$$w = \alpha_0 T\left(-\frac{p_q r^2}{2h} + \frac{p_q z^3}{3h^2} + z\right) + c \qquad (4\text{-}8)$$

The boundary condition at the point $r = 0$ and $z = h$ is $w = 0$. So that

$$w = \alpha_0 T\left(-\frac{p_q r^2}{2h} + \frac{p_q z^3}{3h^2} + z - \frac{hp_q}{3} - h\right) \qquad (4\text{-}9)$$

The optical surface is defined in Equation 3-18. Substituting Equation 3-18 into Equation 4-9 yields

$$w = \alpha_0 T\left[-\frac{p_q r^2}{2h} + p_q\left(\frac{r^2}{2\rho} + \frac{r^4}{4h\rho^2} + \frac{r^6}{24h^3\rho^3}\right) + \frac{r^2}{2\rho}\right] \qquad (4\text{-}10)$$

Results for Case 2. For case 2, the theoretical solution was compared to a numerical solution for two different test cases. Each test case was solved numerically four times, each time with a different number of elements.

Both tests modeled a mirror with a 6:1 diameter-to-thickness ratio. The thermal expansion coefficient at the origin was $23.4 \times 10^{-6}$/K, and the temperature change was 1 K.

Test E is a flat mirror with a 5% change in $\alpha$ from the bottom to the top ($p_q$ = 5%). Test F has a curved optical surface with a radius of curvature, $\rho$, equal to 20 mirror radii. The parameter, $p_q$, is 5%

for Test F.

From Equation 4-6, it can be seen that a flat mirror will deform to a spherical shape provided that the function $\alpha(z)$ is not symmetric about $z = h/2$. Test A from Chapter 3 is a linear case of the function $\alpha(z)$ and the cross-section in Figure 3-3 applies to the quadratic case also.

As in Chapter 3, a point on the outside edge of the mirror surface was chosen to illustrate the comparison. The results of the two tests are shown in Table 4-1. Figures 4-2 and 4-3 are graphs of the percentages that are listed in Table 4-1.

Table 4-1
Results of NASTRAN Models and Theoretical Models

| Test | | Theoretical | NASTRAN | | | |
|---|---|---|---|---|---|---|
| | | | 144 Elements | 300 Elements | 540 Elements | 735 Elements |
| E | Displacement | -1.755 | -1.676 | -1.709 | -1.727 | -1.739 |
| | % of Theoretical | | 95.5 | 97.4 | 98.4 | 99.1 |
| F | Displacement | -1.139 | -1.139 | -1.144 | -1.160 | -1.172 |
| | % of Theoretical | | 97.8 | 100.5 | 101.9 | 102.9 |

Notes: 1. Displacement units are mirror radii times $10^6$
2. Test E -- pq = 5%, rho = $\infty$
3. Test F -- pq = 5%, rho = 20

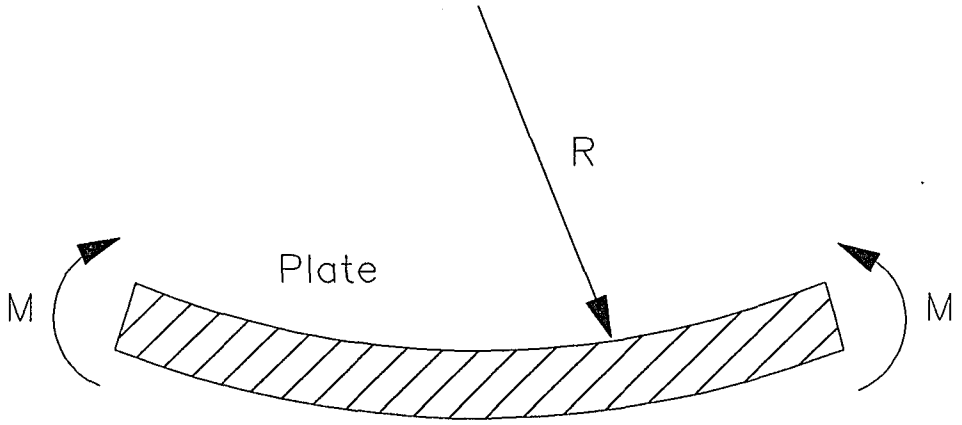


R = Radius of Curvature

M = Applied Moment

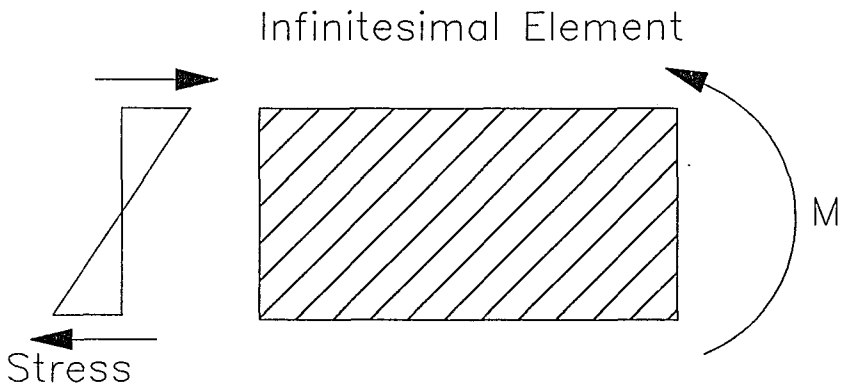


Figure 4–1
Stress and Moment Equilibrium

# Figure 4-2

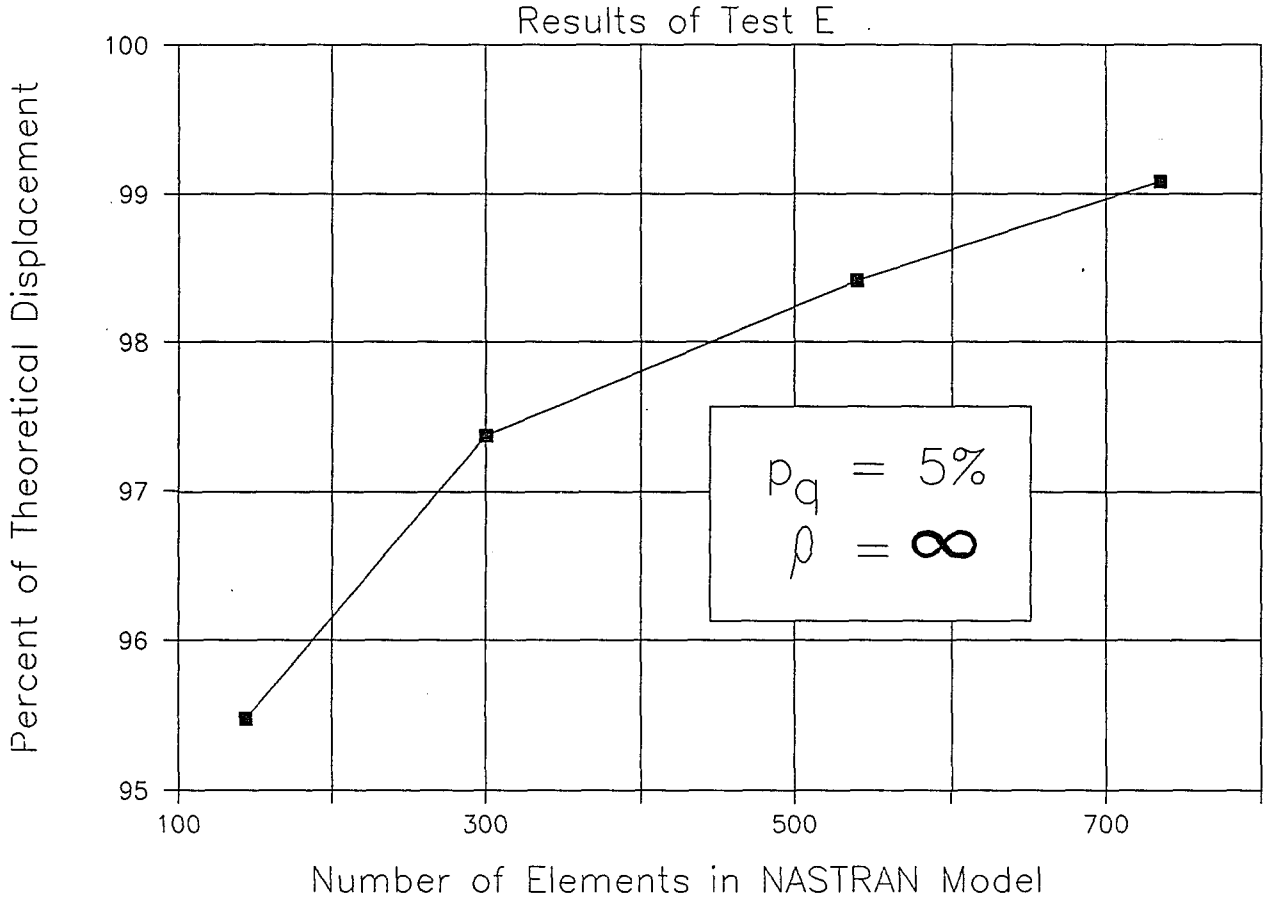
Results of Test E
Percent of Theoretical Displacement
100
99
98
97
96
95
100
300
500
700
Number of Elements in NASTRAN Model
$p_q = 5\%$
$\rho = \infty$

# Figure 4-3

Results of Test F

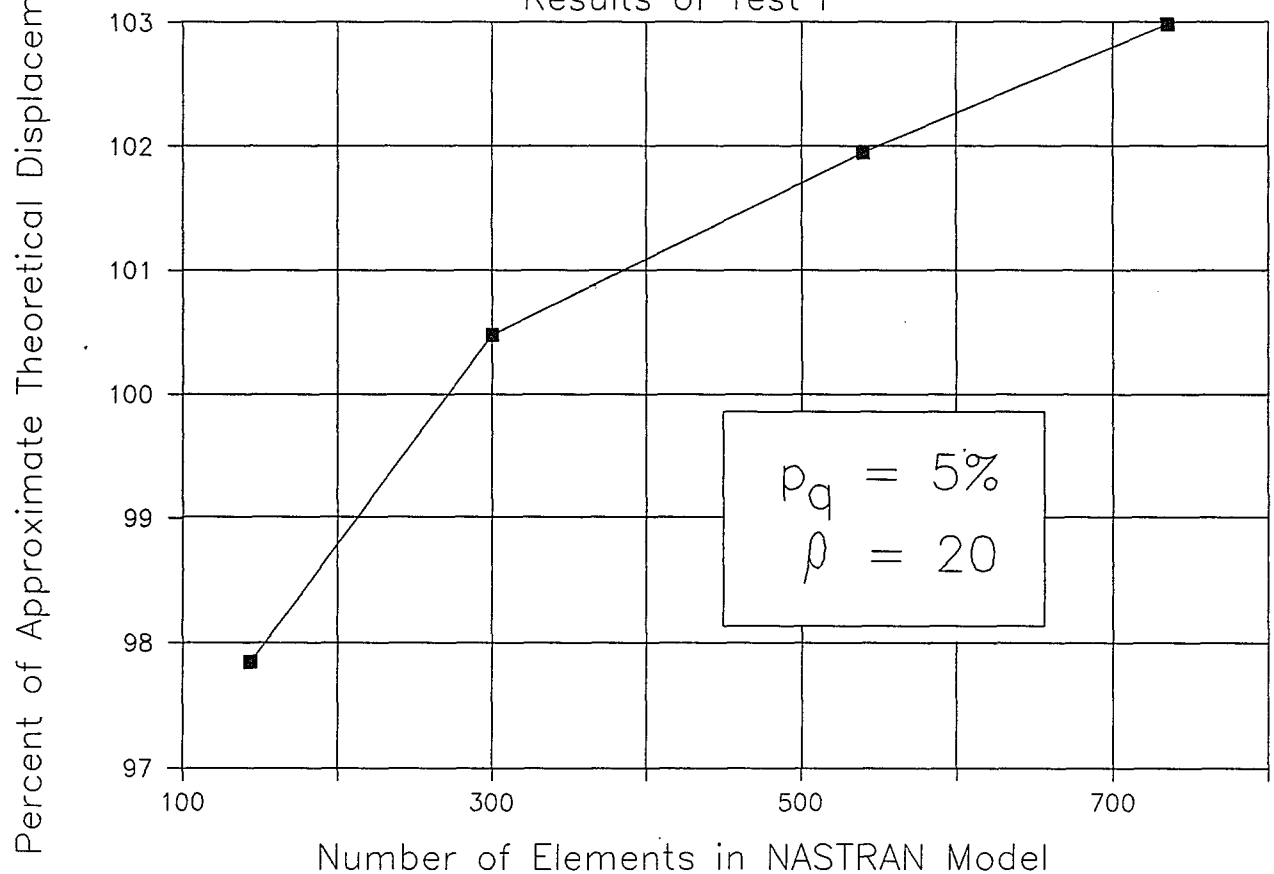

# Chapter 5

## CASE 3: LINEAR VARIATION RADIALLY

The subject of this chapter is the deformations caused by a linear variation in the coefficient of thermal expansion in the radial direction. The chapter is composed of two sections. The first section is a derivation of the displacement equations, and the second section contains the results of a comparison between the theoretically derived model and a finite-element model.

### Derivation

The polar coordinates described in Chapter 2 can conveniently be used for this derivation. The $\alpha(r)T$ distribution -- also described in Chapter 2 -- varies linearly from the center of the mirror to the outside edge. Replace the product $\alpha(r)T$ with $k(r)$, so that

$$k(r) = k_r r + k_0$$

$$\text{where:} \quad k_r = \rho_r \alpha_0 T \tag{5-1}$$

$$k_0 = \alpha_0 T$$

Assume that there is only plane stress, so $\sigma_z = 0$, and $\sigma_r$ and $\sigma_\theta$ must satisfy the equilibrium equation

$$\frac{\partial}{\partial r}\sigma_r + \frac{\sigma_r - \sigma_\theta}{r} = 0 \tag{5-2}$$

Because of axial symmetry, displacements in the $\theta$-direction as well as the shear stresses are zero. Therefore the stress-strain relation is

$$\varepsilon_r = \frac{1}{E}(\sigma_r - \mu\sigma_\theta) + k(r) \tag{5-3}$$

$$\varepsilon_\theta = \frac{1}{E}(\sigma_\theta - \mu\sigma_r) + k(r) \tag{5-4}$$

Solving Equations 5-3 and 5-4 for the stresses, we have

$$\sigma_r = \frac{E}{1-\mu^2}[\varepsilon_r + \mu\varepsilon_\theta - (1+\mu)\,k(r)] \tag{5-5}$$

$$\sigma_\theta = \frac{E}{1-\mu^2}[\varepsilon_\theta + \mu\varepsilon_r - (1+\mu)\,k(r)] \tag{5-6}$$

The strains and the coefficient of thermal expansion are functions of only $r$. Substituting Equations 5-5 and 5-6 into the equilibrium equation yields

$$r\frac{d}{dr}(\varepsilon_r + \mu\varepsilon_\theta) + (1-\mu)(\varepsilon_r - \varepsilon_\theta) = (1+\mu)r\frac{d}{dr}k(r) \tag{5-7}$$

The strain-displacement equations in polar coordinates are

$$\varepsilon_r = \frac{\partial u_r}{\partial r}$$

$$\varepsilon_\theta = \frac{1}{r}\frac{\partial u_\theta}{\partial r} + \frac{u_r}{r} \tag{5-8}$$

Substituting Equation 5-8 into Equation 5-7 results in

$$\frac{d^2}{dr^2} u_r + \frac{1}{r} \frac{d}{dr} u_r - \frac{u_r}{r^2} = (1 + \mu) \frac{d}{dr} k(r) \tag{5-9}$$

Using the product rule, this is rewritten

$$\frac{d}{dr} \left[ \frac{1}{r} \frac{d}{dr} (u_r r) \right] = (1 + \mu) \frac{d}{dr} k(r) \tag{5-10}$$

Integrating Equation 5-10 twice gives

$$u_r = (1 + \mu) \left( \frac{k_r r^2}{3} + \frac{k_0 r}{2} \right) + ar + \frac{b}{r} \tag{5-11}$$

where $a$ and $b$ are constants of integration. The constant $b$ must be zero so that the $r$ displacement is zero along the $z$ axis of the mirror.

After substituting Equation 5-11 into the strain-displacement equations, the strains are

$$\varepsilon_r = (1 + \mu) \left( \frac{2}{3} k_r r + \frac{1}{2} k_0 \right) + a \tag{5-12}$$

$$\varepsilon_\theta = (1 + \mu) \left( \frac{1}{3} k_r r + \frac{1}{2} k_0 \right) + a \tag{5-13}$$

Substituting these equations into the stress-strain equations, we have

$$\sigma_r = - E\left( \frac{1}{3} k_r r + \frac{1}{2} k_0 - \frac{a}{1-\mu} \right) \tag{5-14}$$

$$\sigma_\theta = - E\left( \frac{2}{3} k_r r + \frac{1}{2} k_0 - \frac{a}{1-\mu} \right) \tag{5-15}$$

At the boundary, $r = 1$, the radial stress, $\sigma_r$, must be zero. Substituting these values into Equation 5-14 results in

$$0 = -E\left( \frac{1}{3} k_r + \frac{1}{2} k_0 - \frac{a}{1-\mu} \right) \tag{5-16}$$

Therefore, the constant $a$ is given by

$$a = (1 - \mu)\left( \frac{1}{3} k_r + \frac{1}{2} k_0 \right) \tag{5-17}$$

Now the stresses and the displacement are

$$\sigma_r = E\left( - \frac{1}{3} k_r r + \frac{1}{3} k_r \right) \tag{5-18}$$

$$\sigma_\theta = E\left( - \frac{2}{3} k_r r + \frac{1}{3} k_r \right) \tag{5-19}$$

$$u_r = (1 + \mu)\left( \frac{1}{3} k_r r^2 + \frac{1}{2} k_0 r \right) - (1 - \mu)\, r \left( \frac{1}{3} k_r + \frac{1}{2} k_0 \right) \tag{5-20}$$

The displacement along the optical axis must also be considered. The relation between the stress and the strain in the $z$ direction is

$$\varepsilon_z = -\frac{\mu}{E}(\sigma_r + \sigma_\theta) + k(r) \tag{5-21}$$

Substituting the stresses from Equations 5-18 and 5-19 into Equation 5-21 yields

$$\varepsilon_z = \mu\left(k_r r - \frac{2}{3}k_r\right) + k_r r + k_0 \tag{5-22}$$

The $z$ displacement, is found by integrating Equation 5-22 with respect to $x$. The result is

$$u_z = \left[(1+\mu)k_r r - \mu\frac{2}{3}k_r + k_0\right]z + f(r) \tag{5-23}$$

Because of the imposed condition of plane stress, the shear strain, $\varepsilon_{rz}$ should be zero throughout the mirror. The shear strain as a function of the displacement is

$$\varepsilon_{rz} = \frac{1}{2}\left(\frac{\partial u_r}{\partial z} + \frac{\partial u_z}{\partial r}\right) \tag{5-24}$$

Substituting Equations 5-20 and 5-23 into Equation 5-24 yields

$$\varepsilon_{rz} = \frac{1}{2}\left((1+\mu)k_r z + f'(r)\right) \tag{5-25}$$

Equation 5-25 cannot be true for all $z$. The equation can be satisfied if a single value is chosen for $z$. If $z = h/2$ is chosen this forces the plane halfway through the mirror thickness to move as a rigid body. The resulting equation is

$$\left.\frac{\partial u_z}{\partial r}\right|_{z=\frac{h}{2}} = 0 = (1 + \mu)k_r \frac{h}{2} + f'(r) \qquad (5\text{-}26)$$

Solving for $f'(r)$ and integrating the result with respect to $r$ yields

$$f(r) = \frac{-(1+\mu)k_r h}{2} r + c \qquad (5\text{-}27)$$

where $c$ is a constant of integration to be found by applying the boundary conditions.

Substituting this result into Equation 5-23, the $z$ displacement is

$$u_z = \left[(1+\mu)k_r r - \mu \frac{2}{3} k_r + k_0\right] z - \frac{(1+\mu)k_r h}{2} r + c \qquad (5\text{-}28)$$

Comparison with the Finite-Element Solution

To check the accuracy of the theoretical model, two sample models were solved using the theoretical solution and a NASTRAN finite-element solution.

The finite-element mesh and the boundary conditions were the same as in Chapter 3, except that only one layer of elements was used to represent the thickness.

Boundary Condition. To compare the theoretical model with the finite-element model, the value of c in Equation 5-28 is needed. The boundary condition is zero displacement at the center of the optical surface. Substituting $r$=0, $z$=h, and $u_z$=0 into Equation 5-28 results in

$$c = (\mu \frac{2}{3} k_r - k_0)h \tag{5-29}$$

Defining the Mirror Surface. The mirror surface is defined by Equation 3-18. Combining Equations 5-29, 5-28, and 3-18 yields

$$u_z = \left[(1+\mu)k_r r - \mu \frac{2}{3} k_r r + k_0\right]\left(h + \frac{r^2}{2\rho}\right) \tag{5-30}$$

$$- \frac{1}{2} (1+\mu)k_r hr + (\mu \frac{2}{3} k_r - k_0)h$$

Equation 5-30 is the $z$ displacement of the mirror surface as a function of $r$.

Results for Case 3. To test the theoretical solution, the theoretical solution was compared to a numerical solution for two test cases. Using NASTRAN, each of the test cases was solved four times, increasing the number of elements each time.

All four tests modeled a mirror with a 6:1 diameter-to-thickness ratio. The thermal expansion coefficient at the origin was $23.4 \times 10^{-6}/K$, and the temperature change was 1 $K$.

For tests G and H, $p_r$ = 5%. The axial radius, $\rho$, was infinity for

test G and 20 mirror radii for test H.

Figure 5-1 is a drawing of the cross-section of a mirror that has undergone displacements caused by a linear variation of $\alpha$ along the $r$ axis.

The results of the two theoretical solutions and eight numerical solutions are shown in Table 5-1. The displacements listed are of a point on the outside edge of the mirror surface. Under each displacement, Table 5-1 contains the percentage of the theoretical solution that the displacement represents.

Figures 5-2 and 5-3 contain graphs of the percentages listed in Table 5-1.

Table 5-1
Results of NASTRAN Models and Theoretical Models

| Test | | Theoretical | NASTRAN | | | |
|---|---|---|---|---|---|---|
| | | | 144 Elements | 300 Elements | 540 Elements | 735 Elements |
| G | Displacement | 2.535 | 2.507 | 2.512 | 2.515 | 2.518 |
| | % of Theoretical | | 98.9 | 99.0 | 99.2 | 99.3 |
| H | Displacement | 8.707 | 8.360 | 8.354 | 8.352 | 8.351 |
| | % of Theoretical | | 95.9 | 95.9 | 95.9 | 95.9 |

Notes: 1. Displacement units are mirror radii times $10^7$
2. Test G -- pr = 5%, rho = $\infty$
3. Test H -- pr = 5%, rho = 20

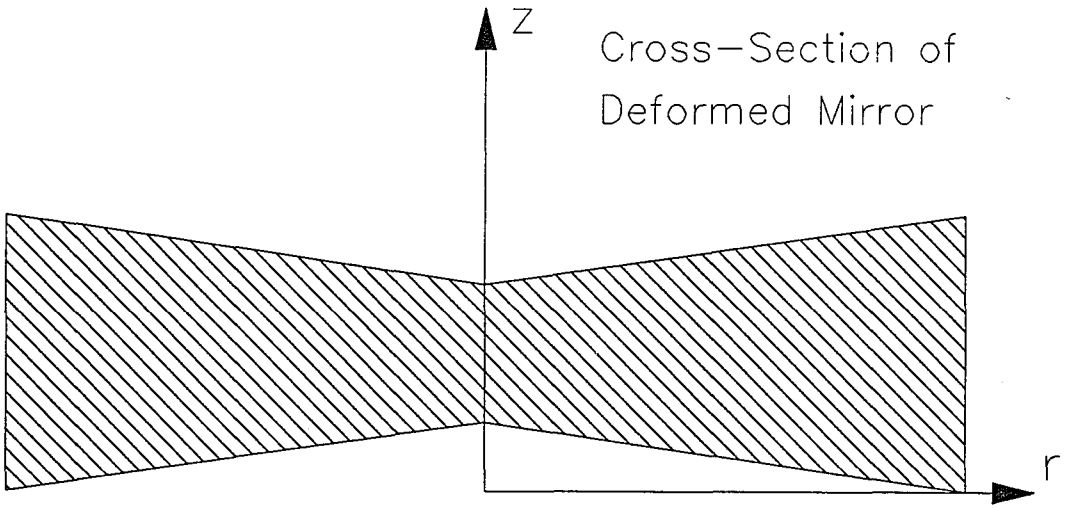


Figure 5–1
Deformation Due to Radial Variation

# Figure 5-2

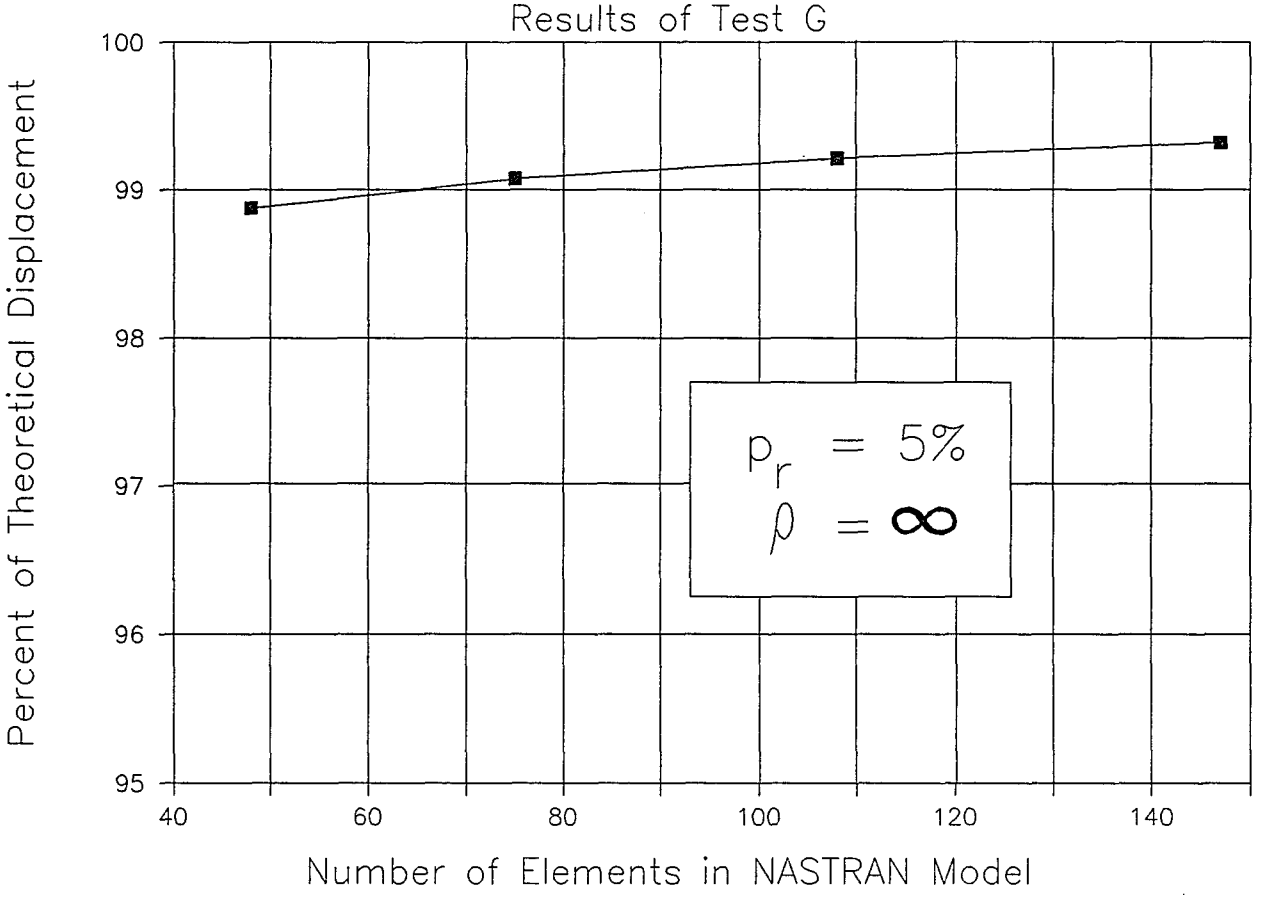
Results of Test G
Percent of Theoretical Displacement
100
99
98
97
96
95
40
60
80
100
120
140
Number of Elements in NASTRAN Model
$p_r = 5\%$
$\rho = \infty$

# Figure 5-3

Results of Test H

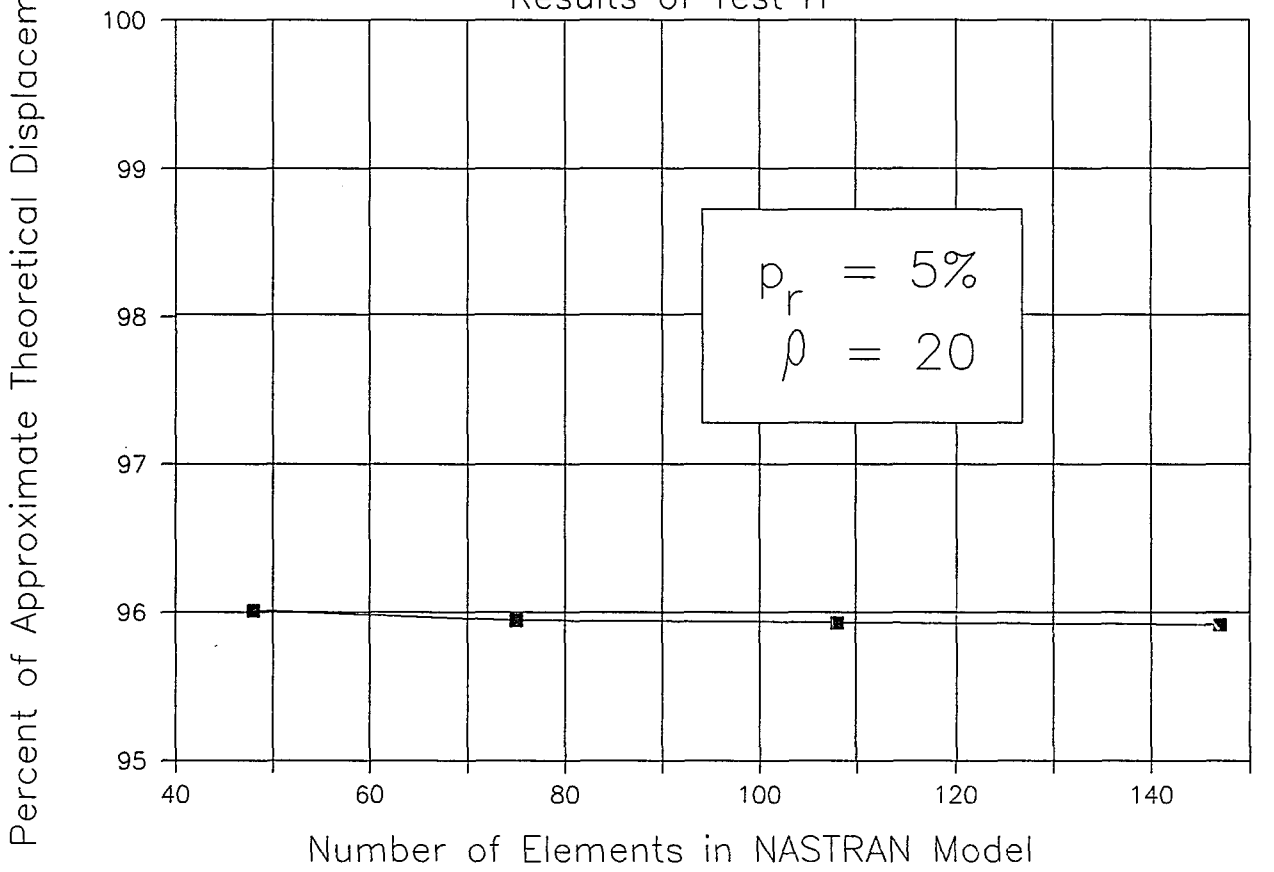

# Chapter 6

## CASE 4: OFF CENTER, RADIAL VARIATION

The subject of this chapter is the displacements caused by a radial variation in the thermal expansion coefficient which proceeds from a point that is not at the center of the mirror (Figure 2.3). Unlike the previous three cases, the function describing the displacement is derived empirically. The first section of the report is a discussion of the derivation of the displacement equation. The second section is a presentation of the results from a finite-element model and from the derived model.

### Derivation

From Chapter 2, the function $\alpha(x,y)$ is

$$\alpha(x,y) = \alpha_0\left\{1 + P_\delta\left[((x+\delta)^2 - y^2)^{1/2} - \delta\right]\right\} \qquad (6\text{-}1)$$

Assume that the $z$ displacement is some multiple of the function $\alpha$ which depends on the parameter $\delta$ (Figure 2.3). The displacement function would also need to include the mirror thickness, $h$, Poisson's ratio, $\mu$, and the temperature change, $T$. One possible function is

$$w = \alpha_0 Th(1 + \mu f(\delta))\alpha(x,y) + c \qquad (6\text{-}2)$$

where $c$ is a rigid body displacement which can be found by

applying the boundary conditions.

It is necessary to find the function $f(\delta)$ to fit the data supplied by the finite-element models.

The function $f(\delta)$ must meet some known conditions at the end points. When $\delta$ is zero, the thermal expansion coefficient has the same distribution as that of Case 3. So the displacement equation should match Equation 5.28 when $\delta$ is zero. As $\delta$ goes to infinity, the distribution of the thermal expansion coefficient is like that of case 1, for $p_y = p_z = 0$, and $p_x = p_\delta$. So the displacement equation should match Equation 3.11 as $\delta$ goes to infinity. To meet these conditions, when $\delta$ is zero, $f(\delta)$ is one, and as $\delta$ goes to infinity, $f(\delta)$ goes to zero.

A possible form for $f(\delta)$ is

$$f(\delta) = (\delta+1)^{-b} \qquad (6\text{-}3)$$

where $b$ is found using linear regression on data from the finite-element models.

The linear curve fit was done on the displacement of one point from eight different mirror models. The point chosen was node seven as shown in Figure 6-1. The eight finite-element models were the same except that the value of $\delta$ was doubled for each successive model, starting at $\delta = 1/8$ up to $\delta = 32$.

The linear regression resulted in $b = 1.409$. Figure 6-2 is a plot of the displacements of node seven from the derived function and from the finite element program versus the parameter $\delta$.

The resulting displacement equation with the boundary conditions applied is

$$w = \alpha_0 Th(1+\mu(\delta+1)^{-b})\{1+p_\delta[((x+\delta)^2+y^2)^{1/2}-\delta]\} \qquad (6\text{-}4)$$

Results

To compare the derived solution with the finite-element solution, 61 nodes were examined for each value of $\delta$ tested. The 61 nodes cover one-half of the mirror's surface.

A comparison of the displacements of the 61 nodes is shown in Figures 6-3 through 6-10. The shaded bars are the $z$-displacements that were predicted by the finite-element models. The cross-hatched bars are the displacements that were predicted by Equation 6-4.

For values of $\delta$ less than two, the derived solution does not match the numerical solution for all of the nodes. This can be seen in Figures 6-3 through 6-6. The assumption that the displacement is some multiple of the $\alpha$ variation appears to be wrong for some range of $\delta$ values.

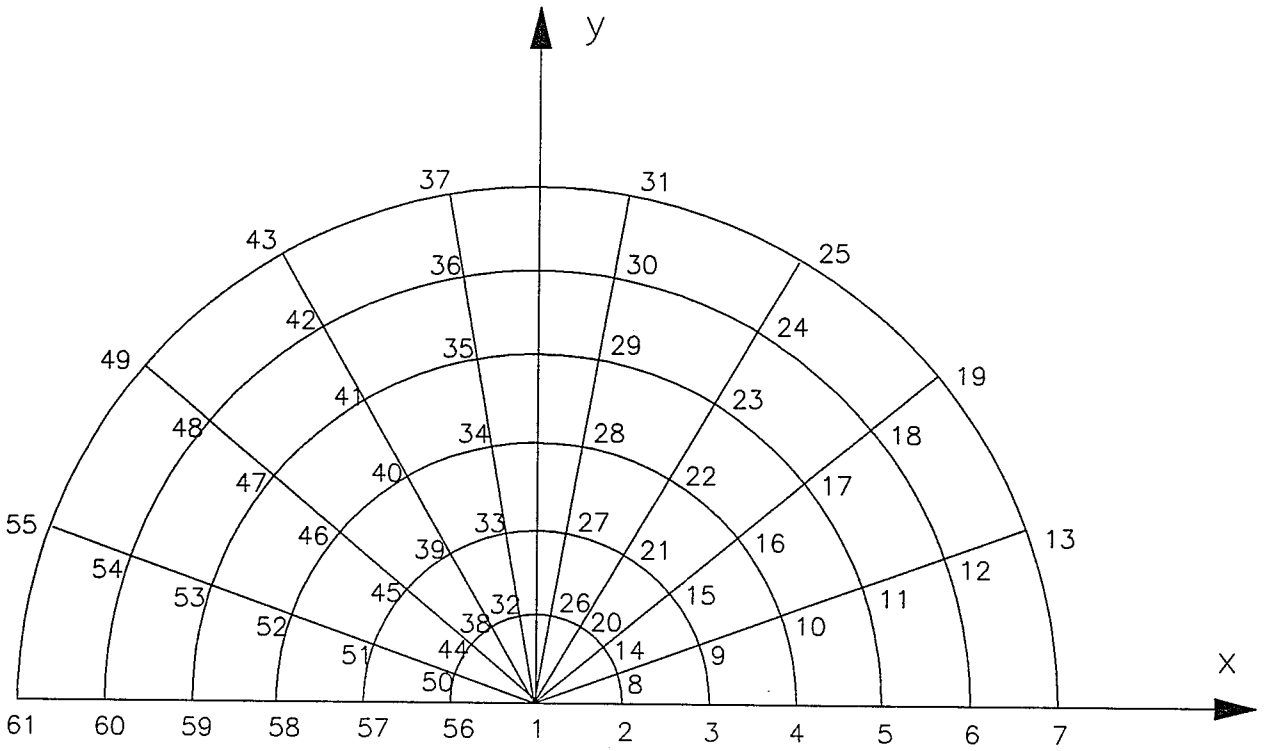


Figure 6–1
Node Numbers

# Figure 6-2

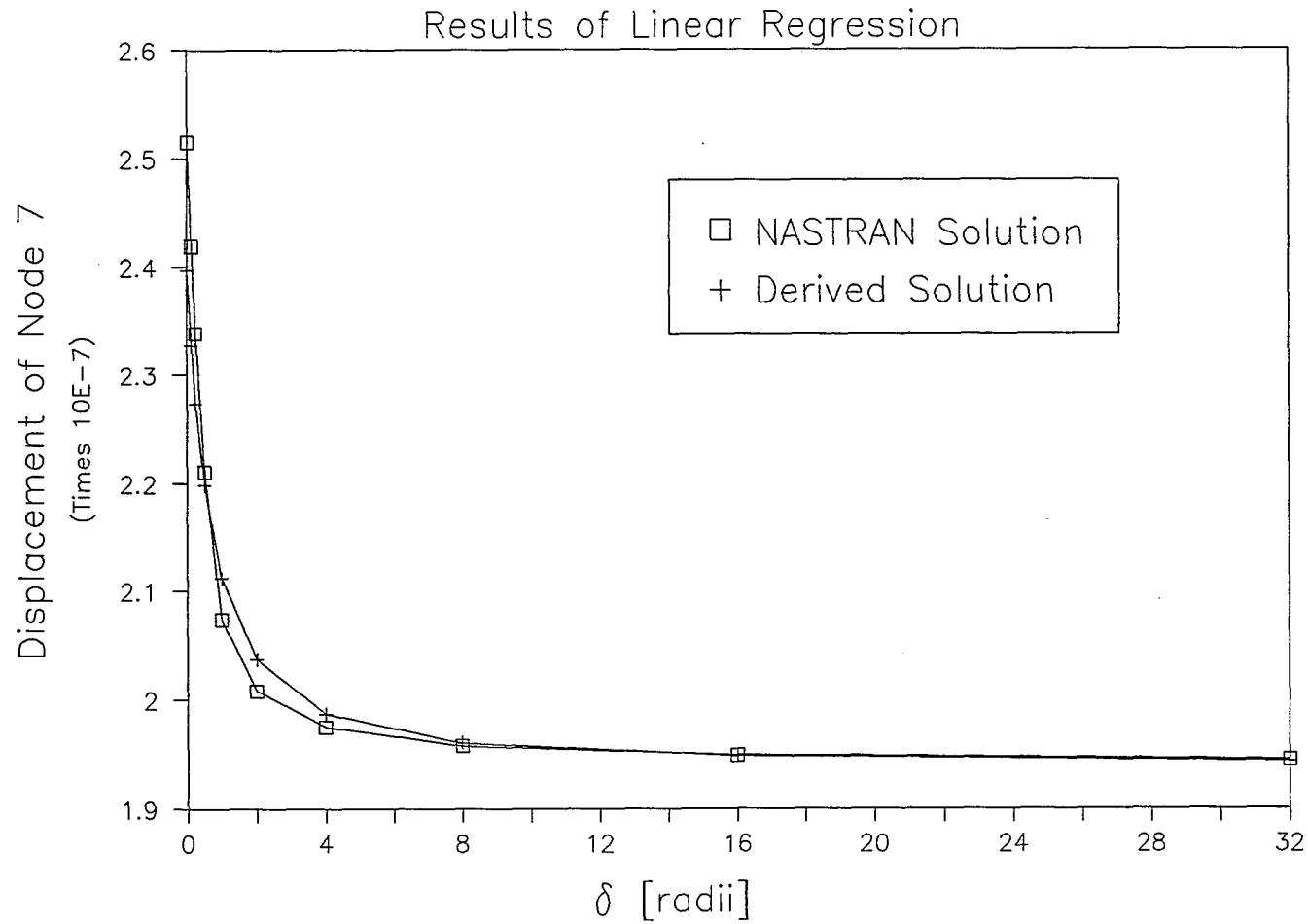
Results of Linear Regression
Displacement of Node 7
(Times 10E-7)
2.6
2.5
2.4
2.3
2.2
2.1
2
1.9
0
4
8
12
16
20
24
28
32
δ [radii]
NASTRAN Solution
Derived Solution

# Figure 6-3

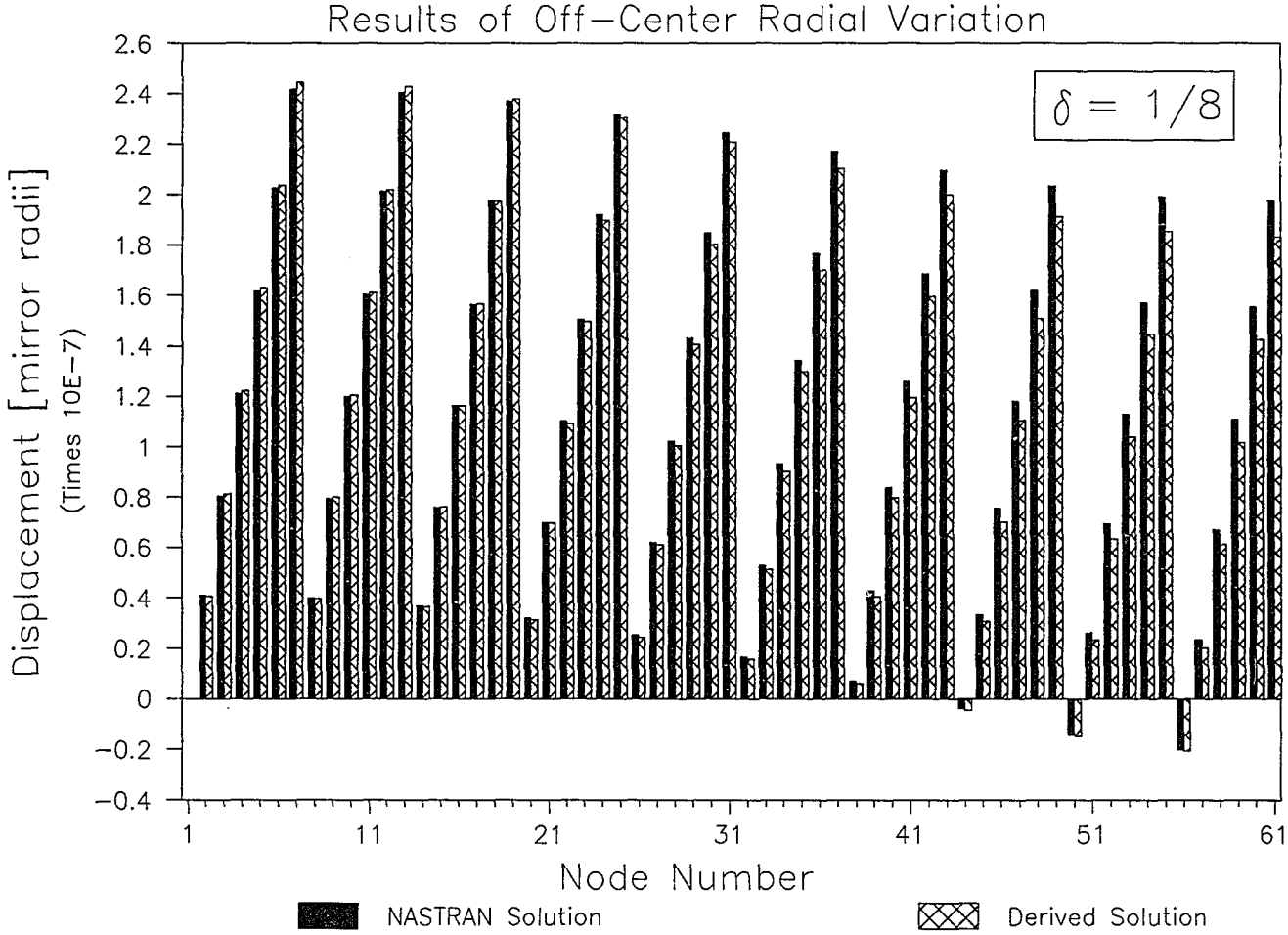
Results of Off-Center Radial Variation
δ = 1/8
Displacement [mirror radii]
(Times 10E-7)
2.6
2.4
2.2
2
1.8
1.6
1.4
1.2
1
0.8
0.6
0.4
0.2
0
-0.2
-0.4
1
11
21
31
41
51
61
Node Number
NASTRAN Solution
Derived Solution

# Figure 6-4

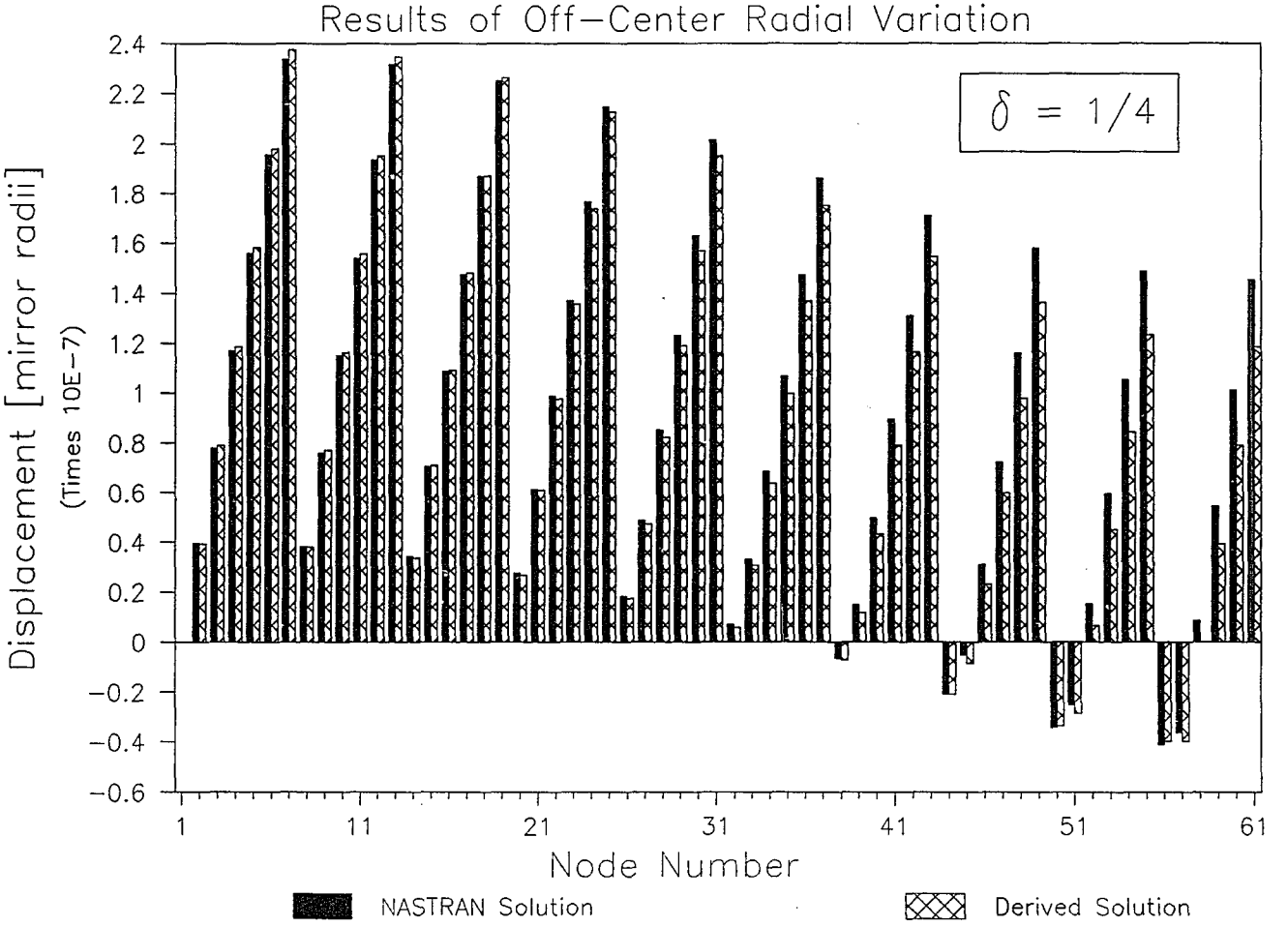
Results of Off-Center Radial Variation
δ = 1/4
Displacement [mirror radii]
(Times 10E-7)
2.4
2.2
2
1.8
1.6
1.4
1.2
1
0.8
0.6
0.4
0.2
0
-0.2
-0.4
-0.6
1
11
21
31
41
51
61
Node Number
NASTRAN Solution
Derived Solution

# Figure 6-5

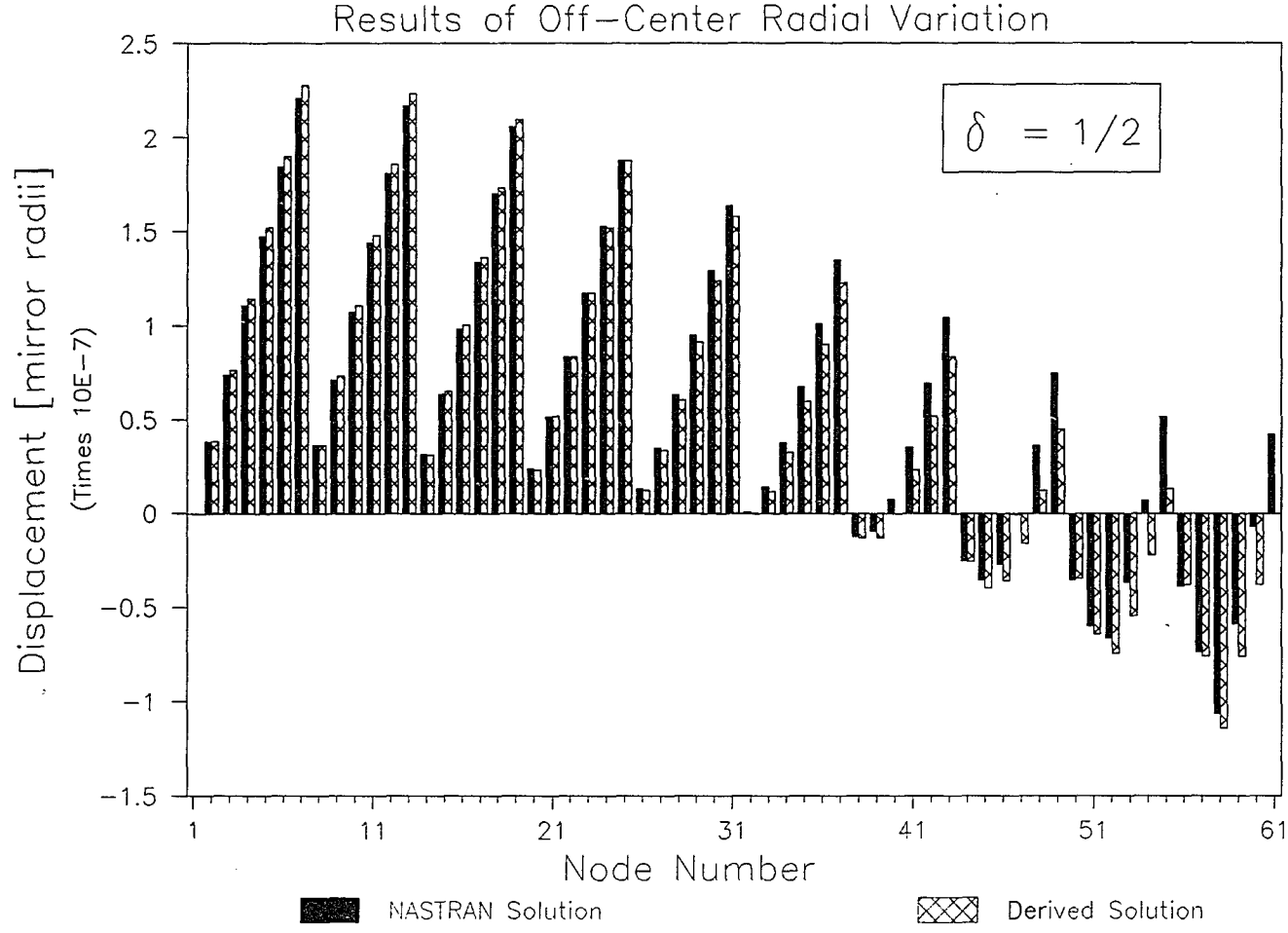
Results of Off-Center Radial Variation
δ = 1/2
Displacement [mirror radii]
(Times 10E-7)
2.5
2
1.5
1
0.5
0
-0.5
-1
-1.5
1
11
21
31
41
51
61
Node Number
NASTRAN Solution
Derived Solution

# Figure 6-6

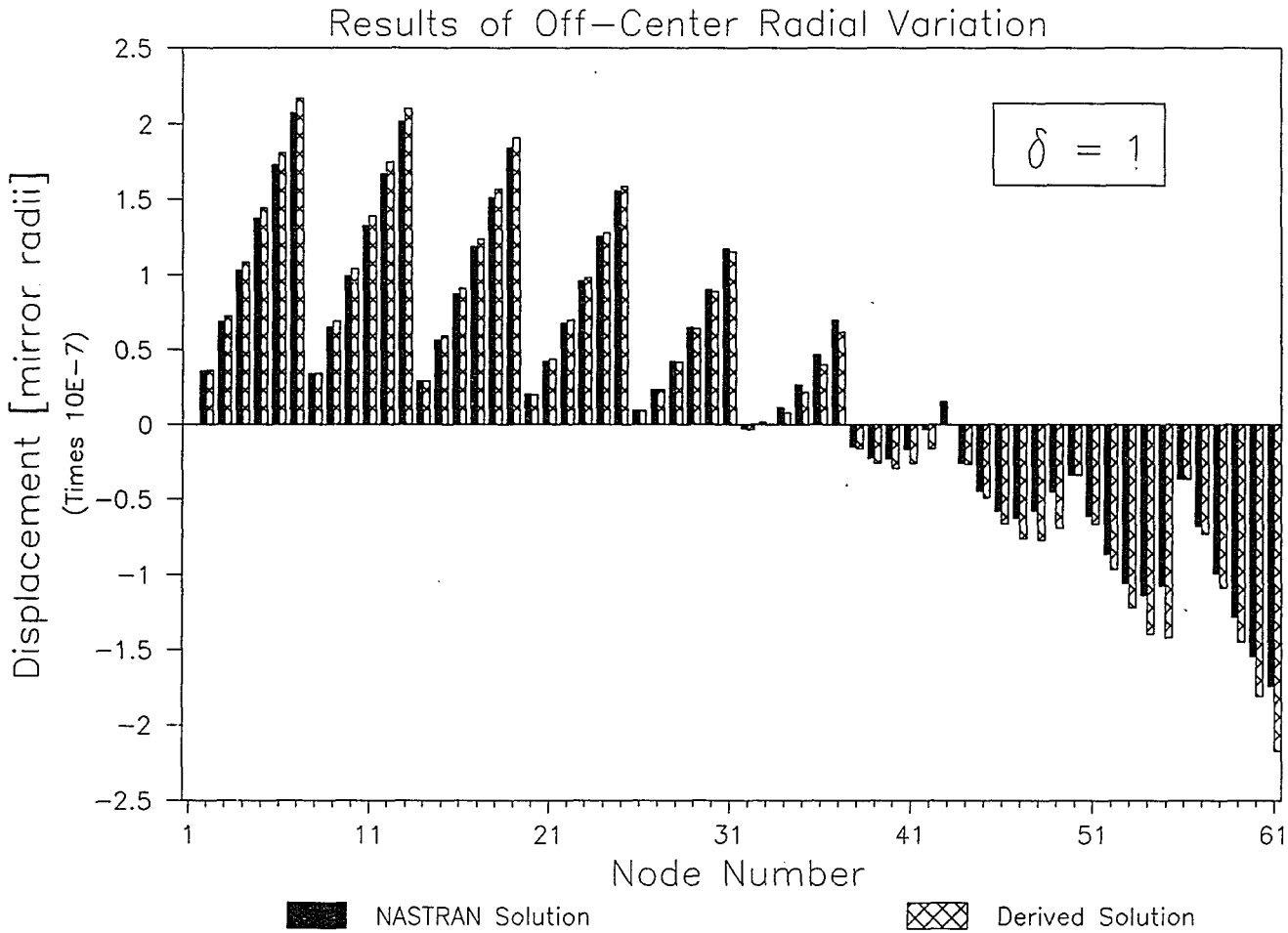
Results of Off-Center Radial Variation
δ = 1
Displacement [mirror radii]
(Times 10E-7)
2.5
2
1.5
1
0.5
0
-0.5
-1
-1.5
-2
-2.5
1
11
21
31
41
51
61
Node Number
NASTRAN Solution
Derived Solution

# Figure 6-7

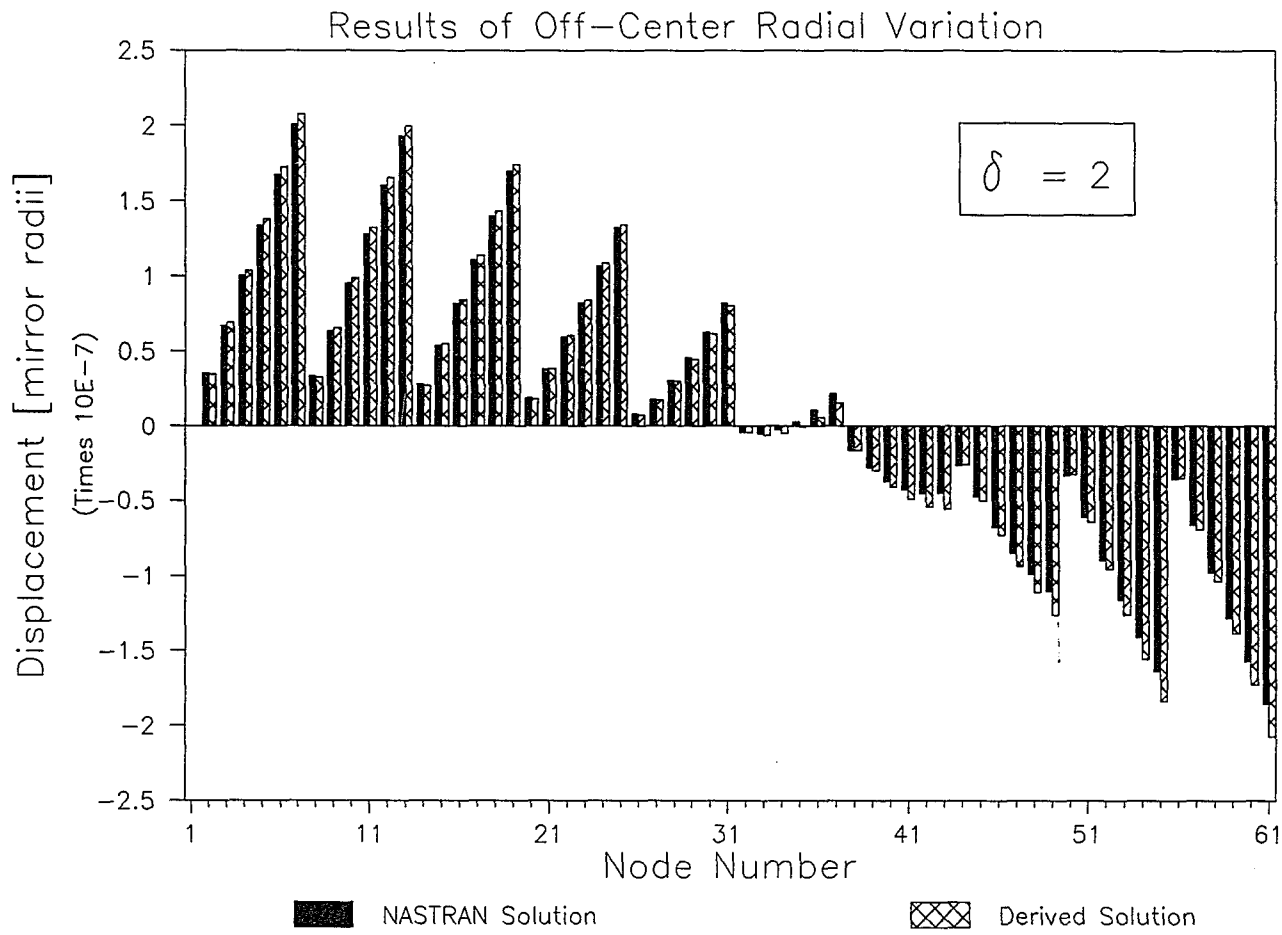
Results of Off-Center Radial Variation
δ = 2
Displacement [mirror radii]
(Times 10E-7)
2.5
2
1.5
1
0.5
0
-0.5
-1
-1.5
-2
-2.5
1
11
21
31
41
51
61
Node Number
NASTRAN Solution
Derived Solution

# Figure 6-8

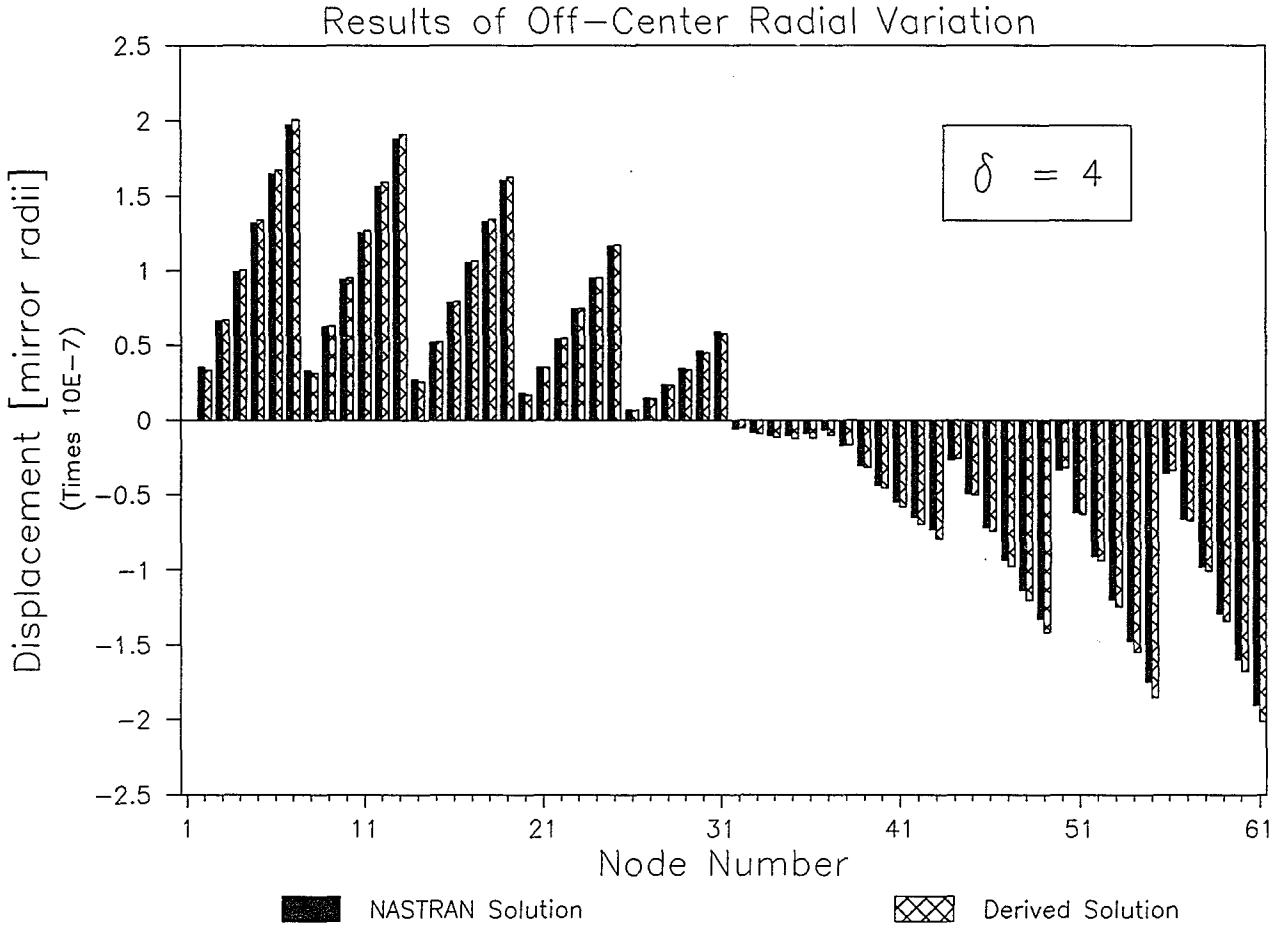
Results of Off-Center Radial Variation
δ = 4
Displacement [mirror radii]
(Times 10E-7)
2.5
2
1.5
1
0.5
0
-0.5
-1
-1.5
-2
-2.5
1
11
21
31
41
51
61
Node Number
NASTRAN Solution
Derived Solution

# Figure 6-9

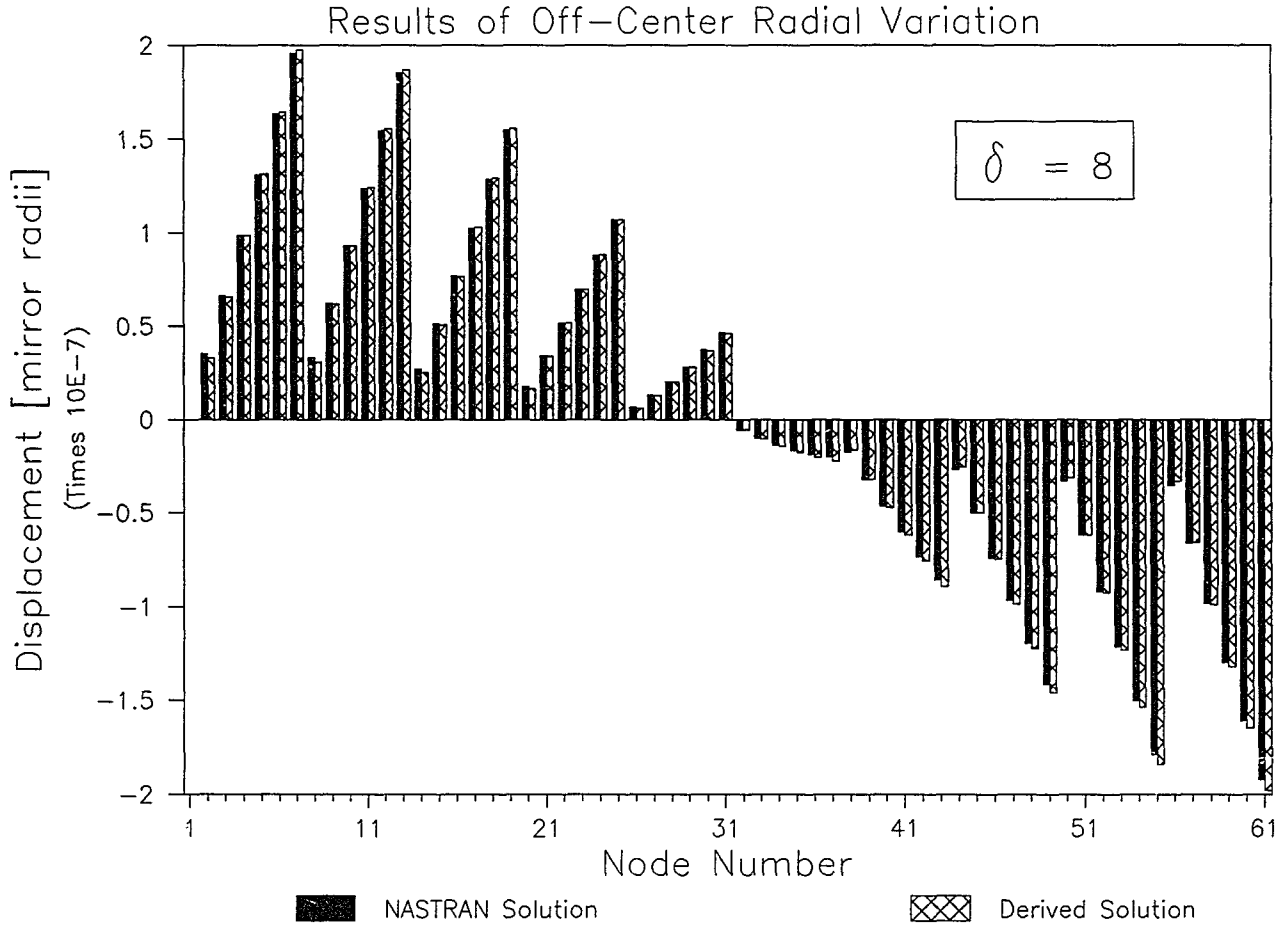
Results of Off-Center Radial Variation
δ = 8
Displacement [mirror radii]
(Times 10E-7)
2
1.5
1
0.5
0
-0.5
-1
-1.5
-2
1
11
21
31
41
51
61
Node Number
NASTRAN Solution
Derived Solution

# Figure 6-10

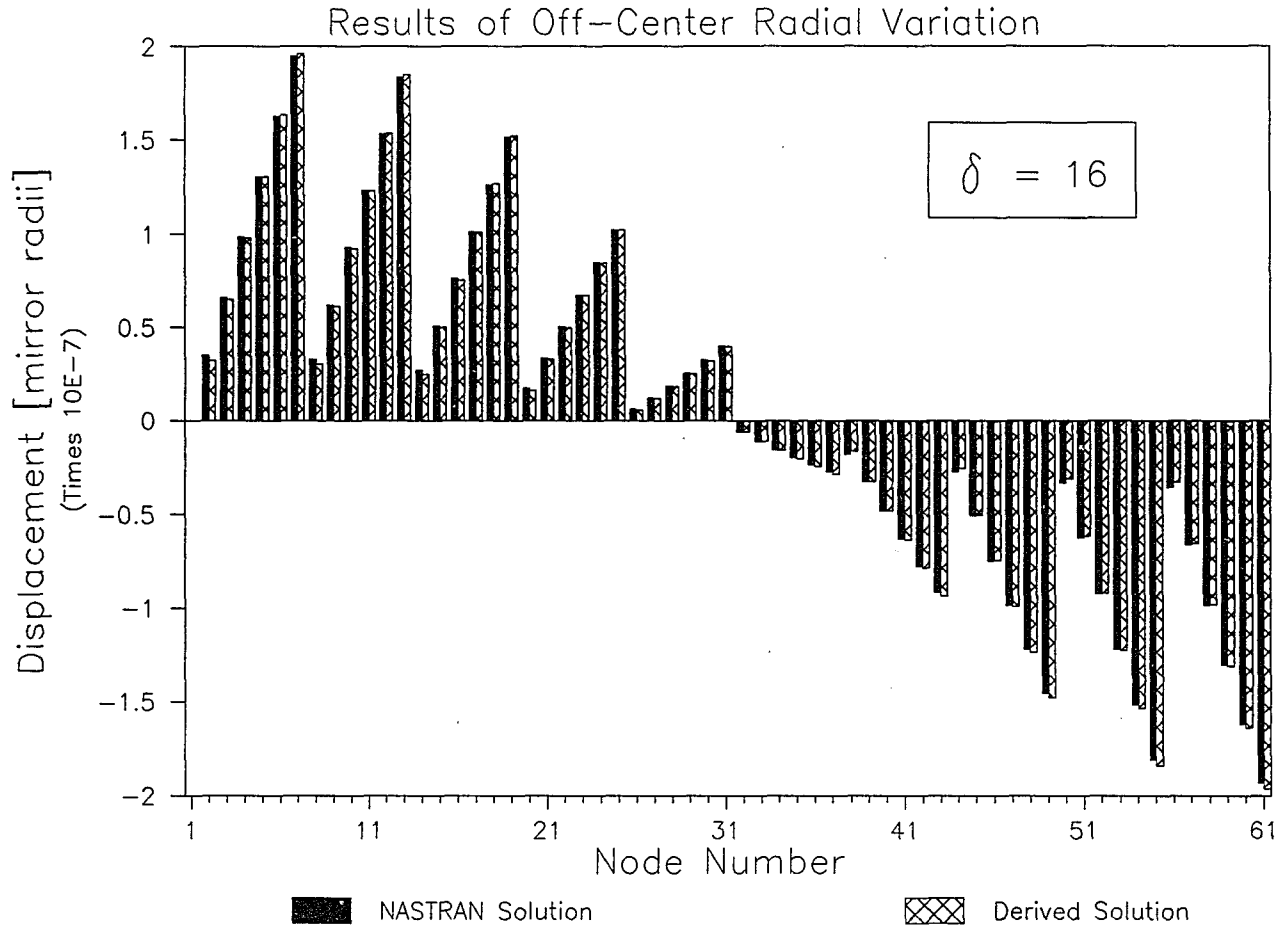
Results of Off-Center Radial Variation
δ = 16
Displacement [mirror radii]
(Times 10E-7)
2
1.5
1
0.5
0
-0.5
-1
-1.5
-2
1
11
21
31
41
51
61
Node Number
NASTRAN Solution
Derived Solution

# Figure 6-11

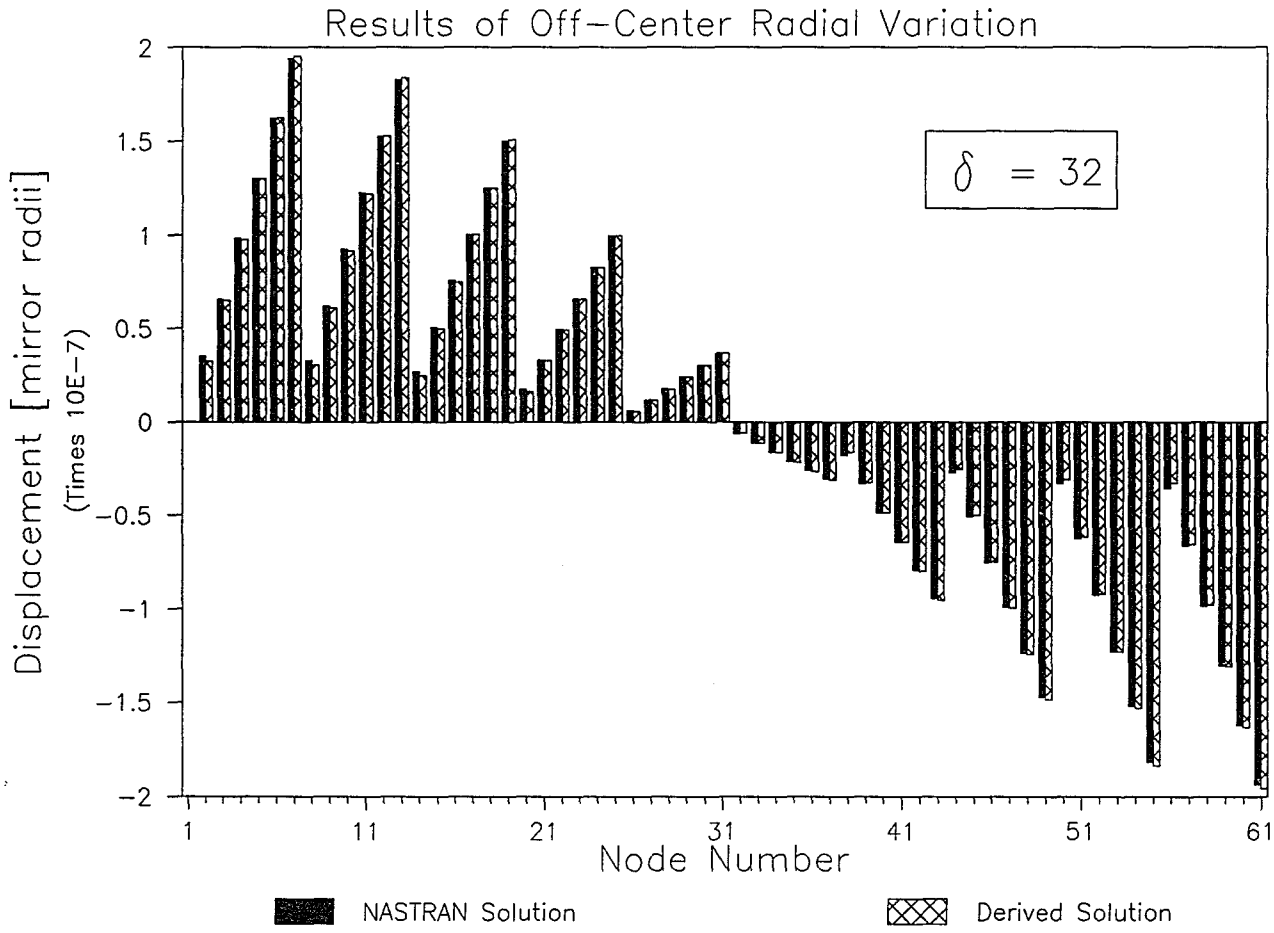
Results of Off-Center Radial Variation
δ = 32
Displacement [mirror radii]
(Times 10E-7)
2
1.5
1
0.5
0
-0.5
-1
-1.5
-2
1
11
21
31
41
51
61
Node Number
NASTRAN Solution
Derived Solution

# Chapter 7

## FUTURE WORK

This chapter is a description of some studies that could be undertaken as an extension of the work described in this thesis. These studies can be divided into two categories: (1) improving the theoretical models for the displacements, and (2) using the displacement models to predict optical aberrations.

### Improving the Displacement Models

The accuracy of the four models derived in this study is lower when the mirror has a curved optical surface. The derivations were all done on flat mirrors and the curvature terms were added merely to account for the expansion of the extra material. Some improvements could be made in this area, but the deviation of the theoretical models from the NASTRAN models was usually within five percent.

Case 4, the off-center, radial variation of $\alpha$, does not match the NASTRAN solution for $\delta$ less than one or two mirror radii. The nodes near the center of the a distribution deviate the greatest amount from the NASTRAN solutions.

### Predicting Optical Aberrations

This study involves mapping the $z$ displacement equations into a Zernike polynomial that describes the deformed surface. The appropriate constants can be extracted from the polynomial and used to

predict aberrations such as tilt, defocus, and astigmatism.

There are two problems with this approach. The first is that the $x$ and $y$ displacements are neglected. For mirrors with low focal numbers, they may contribute to the optical aberrations.

The second problem is that the displacement equations do not map exactly into the Zernike polynomials. Some effort has already been made to do this, but no results have been obtained.

# Appendix A

## Program to Generate the NASTRAN Input File

In this appendix is contained the source code for a program which generates the NASTRAN input file for a mirror with a variation in the thermal expansion coefficient. Instructions for using the program are also included.

### How to use Program Disk

Before running the program, the user must generate a file named header.dat using a text editor. A sample header.dat file is shown in figure A-1. This file contains the machine dependent instructions for running the NASTRAN program, as well as the executive control deck, the CEND card, and the case control deck.

The program generates the BEGIN BULK card, the bulk data deck, and the ENDDATA card. The program combines these cards with the header.dat file and creates the NASTRAN input file.

The program prompts the user with a number of questions regarding the shape of the mirror, the number of elements, and the distribution of the thermal expansion coefficient. The next section contains the questions with which the program prompts the user and some explanation where the prompt may be unclear.

1. **Please enter the name of the NASTRAN input file.**

   The NASTRAN input file is the file that is used to run NASTRAN and is the output from this program.

2. **Please enter the diameter of the mirror.**

   The user may use any units. The output will be in the same units as the mirror diameter.

3. **Please enter the ratio of the diameter to the thickness.**

   After this value is entered, the program will display the thickness of the mirror.

4. **How many layers of elements?**

5. **How many elements radially?**

6. **How many elements around?**

   After these values are entered, the program calculates and displays the total number of elements and nodes in the model.

7. **Please enter the reference temperature.**

   The reference temperature is the temperature at which the mirror was figured.

8. **Enter the axial radius -- rho.**

   Rho is the radius of curvature of the optical surface of the mirror and must have the same units as the diameter. For a flat mirror enter zero.

9. **How many subcases do you want?**

   Because the variation in thermal expansion is modeled using nodal temperatures, a number of loading cases can be used with a single mirror model.

The following questions will be repeated once for each subcase.

10. **Which alpha variation for subcase 1**
    **1. = Linear variation in x y z**
    **2. = Linear radial variation**
    **3. = Quadratic variation in z**
    **4. = Off-center radial variation**

    Choose 1, 2, 3, or 4

11. **Please enter the final temperature.**

    Enter the expected temperature of the mirror during operation.

If 1 is chosen in Question 10, the program asks Question 12.

12. **Enter the percent change in x -- px**
    **Enter the percent change in y -- py**
    **Enter the percent change in z -- pz**

    Enter the value as a percentage, for example, five percent would be entered as 5.

If 2, 3, or 4 is chosen in Question 10, the program asks Question 13.

13. **Enter the percent change in alpha.**

    Enter the value as a percentage.

If 4 is chosen in Question 10, the program asks Question 14.

14. **Enter distance -delta-.**

    This is the amount that the center of the radial distribution of alpha is offset from the center of the mirror.

The program now returns to Questions 10 through 14 to complete the number of subcases requested in Question 9.

The following section contains the source code for program disk.

```
      program disk
*-----------------------------------------------------------------------
c                           Declarations
*-----------------------------------------------------------------------
      implicit double precision (a-h,o-z)
      common radius,thick,percent,tdum,tref
      real tnode(5000),rnode(5000),znode(5000),tfinal(5000)
      integer el(5000,10),edge_hold
      character dummy(5000,10)
      character*30 outfile
      character*80 header(50)


*-----------------------------------------------------------------------
c                             Inputs
*-----------------------------------------------------------------------

c----------------open the output file
      write(6,*)'Please enter the name of the NASTRAN input file.'
      read(5,1000)outfile
1000  format(a)
      write(6,*)
      open(unit=1,file=outfile,status='new')
      open(unit=3,file='header.dat',status='old')
      write(6,*)

c----------------read diameter of disk = diameter
      write(6,*)'Please enter the diameter of the mirror.'
      read(5,*)diameter
      write(6,*)
      radius = diameter/2.0

c----------------read ratio = a
      write(6,*)'Please enter the ratio of diameter to thickness.'
      read(5,*)a
      write(6,*)

c----------------calculate the thickness and output
      thick = diameter/a
      write(6,1001)thick
1001  format(' The thickness is ',f12.6)
      write(6,*)

c----------------read no of layers = nlays
      write(6,*)'How many layers of elements?'
      read(5,*)nlays
      write(6,*)
```

```
c----------------read no of elements radially = nrad
      write(6,*)'How many elements radially?'
      read(5,*)nrad
      write(6,*)

c----------------read no of elements around = ntheta
      write(6,*)'How many elements around?'
      read(5,*)ntheta
      write(6,*)

c----------------calculate the total number of nodes and elements
      nelems = nrad*ntheta*nlays
      nnodes = (nrad*ntheta+1)*(nlays+1)
      write(6,1002)nelems
1002  format(' The total number of elements is ',i5)
      write(6,*)
      write(6,1003)nnodes
1003  format(' The total number of nodes is ',i5)

c----------------get the reference temperature
      write(6,*)
      write(6,*)'Please enter the reference temperature.'
      read(5,*)tref
      write(6,*)

c---------------- get the axial radius -- rho
      write(6,*)'enter the axial radius -- rho'
      read(5,*)rho
      write(6,*)

c----------------calculate the space between nodes
      delt = 360./ntheta
      delr = radius/nrad
      delz = thick/nlays
      ibotcent = 1+(ntheta*nrad+1)*nlays
      iroll1 = ibotcent + 2*nrad/3
      iroll2 = iroll1 + nrad*ntheta/3
      iroll3 = iroll2 + nrad*ntheta/3
      edge_hold = 1 + nrad

*-----------------------------------------------------------------
c                   generate the node data
*-----------------------------------------------------------------
      n = 0
      do 10 i = nlays,0,-1
         n = n+1
         tnode(n) = 0.0
         rnode(n) = 0.0
         znode(n) = float(i)*delz
```

```
         do 10 j = 0,ntheta-1
            do 10 k = 1,nrad
               n = n+1
           tnode(n) = float(j)*delt
           rnode(n) = float(k)*delr
           znode(n) = float(i)*delz
10    continue

c----------------change top layer if mirror is not flat
      if (rho .ne. 0.)then
         do i = 2,nrad*ntheta + 1
            znode(i) = znode(i) + rho -
     &                    sqrt(rho*rho - rnode(i)*rnode(i))
         enddo
      endif

*-----------------------------------------------------------------------
c                  generate the element connectivity
*-----------------------------------------------------------------------
      nepl = nrad*ntheta
      npl  = nepl+1

      n = 0
      do 40 i = 0,nlays-1
         do 30 j = 0,ntheta-2
            n = n+1
            el(n,1) = 1
            el(n,5) = 2 + j*nrad + i*npl
            el(n,6) = el(n,5) + nrad
            el(n,7) = 1 + i*npl
            el(n,2) = el(n,5) + npl
            el(n,3) = el(n,6) + npl
            el(n,4) = el(n,7) + npl
30    continue
      n = n+1
      el(n,1) = 1
      el(n,5) = el(n-1,6)
      el(n,6) = el(n-j,5)
      el(n,7) = el(n-1,7)
      el(n,2) = el(n,5) + npl
      el(n,3) = el(n,6) + npl
      el(n,4) = el(n,7) + npl
```

```
      do 60 j = 0,ntheta-2
         do 60 k = 0,nrad-2
            n = n+1
            el(n,1) = 2
            el(n,6) = 2 + j*nrad + k + npl*i
            el(n,7) = el(n,6) + 1
            el(n,8) = el(n,7) + nrad
            el(n,9) = el(n,8) - 1
            el(n,2) = el(n,6) + npl
            el(n,3) = el(n,7) + npl
            el(n,4) = el(n,8) + npl
            el(n,5) = el(n,9) + npl
60    continue
      do 90 k = 0,nrad-2
        n = n+1
          el(n,1) = 2
          el(n,6) = 2 + j*nrad + k + npl*i
          el(n,7) = el(n,6) + 1
          el(n,8) = 3 + i*npl + k
          el(n,9) = el(n,8) - 1
          el(n,2) = el(n,6) + npl
          el(n,3) = el(n,7) + npl
          el(n,4) = el(n,8) + npl
          el(n,5) = el(n,9) + npl
90    continue

40    continue
      nelems = n

*--------------------------------------------------------------------
c               output the results to a formatted file
*--------------------------------------------------------------------

      nhead = 0
      do 501 n = 1,50
         read(3,500,end=502)header(n)
         nhead = nhead + 1
500      format(a80)
501   continue
502   continue

      do 503 n = 1,nhead
         write(1,504)header(n)
504      format(a80)
503   continue
```

```
      write(1,900)
900   format('BEGIN BULK')
      write(1,901)
901   format('CORD2C,1,0,0.0,0.0,0.0,0.0,0.0,1.0,')
      write(1,902)
902   format(',1.0,0.0,0.0')

      do 100 n = 1,nelems
         if(el(n,1) .eq. 1)then
            write(1,910)n,(el(n,i),i=2,7)
910         format('CPENTA,',I4,',1,',I4,',',I4,',',I4,',',
     &                 I4,',',I4,',',I4)
         else
            write(1,920)n,(el(n,i),i=2,7)
920         format('CHEXA,',I4,',1,',I4,',',I4,',',I4,',',
     &                  I4,',',I4,',',I4,',')
            write(1,930)el(n,8),el(n,9)
930         format(',',I4,',',I4)
            ncont = ncont + 1
         endif
100   continue


      do 110 n = 1,nnodes

         write(1,940)n,rnode(n),tnode(n),znode(n)
940      format('GRID,'i4,',1,',f8.4,',',f8.4,',',f8.4,',1')
110   continue

      write(1,950)tref
950   format('MAT1,1,70.+6,,.3,1.5536,23.4e-6,',f8.4)


      write(1,960)
960   format('PSOLID,1,1')

      write(1,971)edge_hold
      write(1,972)
      write(1,974)ibotcent
974   format('SPC,23,',I4,',12')
972   format('SPC,23,1,123')
971   format('SPC,23,',i4,',2')
      write(1,976)nnodes
976   format('SPC1,23,456,1,THRU,',i4)
```

```
*-----------------------------------------------------------------------
c         generate the temperature load cards for each subcase
*-----------------------------------------------------------------------

      write(6,*)'How many subcases do you want?'
      read(5,*)nsub
      do 2000 j = 1,nsub
         write(6,*)'Which temperature variation for subcase ',j
         write(6,*)'          1 = Linear variation in x y z'
         write(6,*)'          2 = Linear radial variation'
         write(6,*)'          3 = Quadratic variation in z'
         write(6,*)'          4 = Off center radial variation'
         read(5,*)i_tvar



c----------------get the final temperature
         write(6,*)'Please enter the final temperature.'
         read(5,*)tdum
         write(6,*)

         if(i_tvar .eq. 1)then
      write(6,*)'enter the percent difference in x -- px'
      read(5,*)pxd
      write(6,*)'enter the percent difference in y -- py'
      read(5,*)pyd
      write(6,*)'enter the percent difference in z -- pz'
      read(5,*)pzd

      px = .01*pxd
      py = .01*pyd
      pz = .01*pzd

            do 120 n = 1,nnodes
               call linthick(tfinal(n),rnode(n),tnode(n),znode(n)
     &                              ,p1,p2,p3)
120         continue
         elseif(i_tvar .eq. 2)then
c----------------get the percent alpha variation
            write(6,*)'Please enter the percent alpha variation'
            read(5,*)percentd
            percent = percentd*.01
```

```
c----------------fill the temp load cards
            do 121 n = 1,nnodes
               call linrad(tfinal(n),rnode(n),tnode(n),znode(n))
121         continue
         elseif(i_tvar .eq. 3)then
            write(6,*)'Please enter the percent alpha variation'
            read(5,*)percentd
            percent = percentd*.01

c----------------fill the temp load cards
            do 122 n = 1,nnodes
               call quad(tfinal(n),rnode(n),tnode(n),znode(n))
122         continue
         elseif(i_tvar .eq. 4)then
            write(6,*)'Please enter the percent alpha variation'
            read(5,*)percentd
            percent = percentd*.01

c----------------fill the temp load cards
            write(6,*)'Enter distance -delta- '
            read(5,*)delta
            do n = 1,nnodes
             call offcenter(tfinal(n),rnode(n),tnode(n),znode(n),delta)
            enddo
         else
          write(6,*)'That subcase is not available'
             goto 2000
         endif

         do 130 n = 1,nnodes
            write(1,990)j,n,tfinal(n)
990         format('TEMP,',i4,',',I4,',',f8.5)
130      continue
2000  continue

      write(1,980)
980   format('ENDDATA')
      close(1)
      close(2)
      end
```

```
*-----------------------------------------------------------------------
c         generate the temperature load cards for subcase 1
c                    linear variation in x y z
*-----------------------------------------------------------------------

      subroutine linthick(tfinal,r,t,z,p1,p2,p3)
      implicit double precision (a-h,o-z)
      common radius,thick,percent,tdum,tref
      d = radius
      x = r*cos(t/57.29577951)
      y = r*sin(t/57.29577951)
      tfinal = (x*p1/d + y*p2/d + z*p3/thick + 1.)*
     &           (tdum-tref) + tref
      return
      end
```

```
*--------------------------------------------------------------------
c         generate the temperature load cards for subcase 2
c                    linear radial variation
*--------------------------------------------------------------------

      subroutine linrad(tfinal,r,t,z)
      implicit double precision (a-h,o-z)
      common radius,thick,percent,tdum,tref
      tfinal = (1. + (r/radius)*percent)*(tdum-tref) + tref
      return
      end
```

```
*-----------------------------------------------------------------------
c         generate the temperature load cards for subcase 3
c                    quadratic variation in z
*-----------------------------------------------------------------------

      subroutine quad(tfinal,r,t,z)
      implicit double precision (a-h,o-z)
      common radius,thick,percent,tdum,tref
      tfinal = (1. + (z*z/thick/thick)*percent)*(tdum-tref) + tref
      return
      end
```

```
*-----------------------------------------------------------------------
c         generate the temperature load cards for subcase 4
c                    off-center radial variation
*-----------------------------------------------------------------------

      subroutine offcenter(tfinal,r,t,z,a)
      implicit double precision (a-h,o-z)
      common radius,thick,percent,tdum,tref
      x = r*cos(t/57.29577951)
      y = r*sin(t/57.29577951)
      xprime = x + a
      d = sqrt(xprime*xprime + y*y) - a
      tfinal = (1. + (d/radius)*percent)*(tdum-tref) + tref
      return
      end
```

**FIGURE A-1**

**HEADER.DAT**

```
USERNAME,BN1111111X,T900,P0
PW,SECRET
ATTACH,LNKFILE,NASTRANLNKFILE,ID=LWP,MR=1.
ATTACH ,NASTRAN,ID=LWP.
NASTRAN.
GOTO,2.
EXIT(S)
REWIND,OUTPUT.
COPYCF,OUTPUT,X.
REWIND,X.
TOVAX(I=X,FILE=$a4.OUT$,USER=NAME,PW=CODE)
DISPOSE(PUNCH,*SC)
#EOR
ID RUN,THREE
SOL 24
TIME 80
CEND
TITLE = OFF-CENTER TEST
     SPC=23
     ECHO = NONE
     SET 1 = 1 THRU 61
     DISP = 1
SUBCASE 1
     LABEL= A IS 1/8
     TEMP(LOAD)=1
SUBCASE 2
     LABEL= A IS 1/4
     TEMP(LOAD)=2
SUBCASE 3
     LABEL= A IS 1/2
     TEMP(LOAD)=3
SUBCASE 4
     LABEL= A IS 1
     TEMP(LOAD)=4
```

# Appendix B

## Output from Program FRINGE

In this appendix is contained the output from program FRINGE. Given data representing the surface of a mirror, the FRINGE program calculates the coefficients of a Zernike polynomial representing the surface. The program then combines the appropriate terms from the polynomial and calculates the magnitudes of various optical aberrations.

For this appendix, the data representing the mirror surface is from the various displacement models derived in this report. For all the cases the model is of a one-meter diameter mirror simply supported at three points on the bottom surface. The support points are one-half the distance from the center to the outside edge and are 120 degrees apart. The supports allow the mirror model to displace in the x-y plane but not in the z axis.

In tables B-1 through B-11 is contained the output from the FRINGE program. The title block of each table contains a description of the type of variation in the thermal expansion coefficient that is being modeled. The title block also contains the temperature change (T), and the value of the thermal expansion coefficient at the center of the mirror's bottom surface (alpha).

The first column of each table is the percent change in alpha in some direction. A subscript of x denotes the x-direction, z denotes the z-direction, and r denotes the r-direction. The subscript q means

that the change is quadratic along the z axis.

The remaining seven columns are the optical aberrations as reported by the FRINGE program. The units are wavelengths where one wavelength is 3165 angstroms. The abbreviation astig means astigmatism, and the abbreviation sph ab means spherical aberration.

The cases shown in Table B-1 represent a mirror with a constant thermal expansion coefficient throughout the body of the mirror. The temperature change is -10 K.

Tables B-2 through B-7 are from models of a linear variation of the thermal expansion coefficient along one axis of the body. The x axis is along a diameter and the z axis is through the thickness. The origin for all the coordinate systems used is the center of the bottom surface of the mirror.

Tables B-8 and B-9 represent a quadratic variation of the thermal expansion coefficient through the thickness of the mirror.

Tables B-10 and B-11 represent a linear variation of the thermal expansion coefficient along radial lines in the plane of the mirror starting at the origin.

Table B-1 No Alpha Variation T = -10 K alpha = $23.4 \times 10^{-6}$

| p | D/T | Rho | RMS | Span | Tilt | Focus | Astig | Coma | Sph Ab |
|---|---|---|---|---|---|---|---|---|---|
| 0.000 | 6 | Flat | 0.01 | 0.02 | 0.00 | 0.02 | 0.00 | 0.00 | 0.00 |
| 0.000 | 20 | Flat | 0.01 | 0.02 | 0.00 | 0.02 | 0.00 | 0.00 | 0.00 |
| 0.000 | 6 | 1000 | 2.73 | 9.40 | 0.00 | 9.40 | 0.00 | 0.00 | 0.01 |
| 0.000 | 20 | 1000 | 2.70 | 9.29 | 0.00 | 9.29 | 0.00 | 0.00 | 0.01 |
| 0.000 | 10 | Flat | 0.01 | 0.02 | 0.00 | 0.02 | 0.00 | 0.00 | 0.00 |
| 0.000 | 10 | 1000 | 2.71 | 9.34 | 0.00 | 9.34 | 0.00 | 0.00 | 0.01 |
| 0.000 | 6 | 2000 | 1.35 | 4.66 | 0.00 | 4.66 | 0.00 | 0.00 | 0.00 |
| 0.000 | 10 | 2000 | 1.35 | 4.65 | 0.00 | 4.65 | 0.00 | 0.00 | 0.00 |
| 0.000 | 20 | 2000 | 1.34 | 4.63 | 0.00 | 4.63 | 0.00 | 0.00 | 0.00 |

| Table B-2 Linear Variation in the x Direction T = -1 K alpha = $23.4 \times 10^{-6}$ | | | | | | | | | |
|---|---|---|---|---|---|---|---|---|---|
| Px | D/T | Rho | RMS | Span | Tilt | Focus | Astig | Coma | Sph Ab |
| 5.0% | 6 | Flat | 0.14 | 0.62 | 0.29 | 0.00 | 0.00 | 0.03 | 0.00 |
| 1.0% | 6 | Flat | 0.03 | 0.12 | 0.06 | 0.00 | 0.00 | 0.01 | 0.00 |
| 0.5% | 6 | Flat | 0.01 | 0.06 | 0.03 | 0.00 | 0.00 | 0.00 | 0.00 |
| 5.0% | 20 | Flat | 0.04 | 0.19 | 0.07 | 0.00 | 0.00 | 0.03 | 0.00 |
| 1.0% | 20 | Flat | 0.01 | 0.04 | 0.01 | 0.00 | 0.00 | 0.01 | 0.00 |
| 0.5% | 20 | Flat | 0.00 | 0.02 | 0.01 | 0.00 | 0.00 | 0.00 | 0.00 |
| 5.0% | 6 | 1000 | 14.76 | 79.88 | 19.86 | 0.94 | 0.00 | 31.48 | 0.00 |
| 1.0% | 6 | 1000 | 2.96 | 15.98 | 3.97 | 0.94 | 0.00 | 6.30 | 0.00 |
| 0.5% | 6 | 1000 | 1.50 | 7.99 | 1.99 | 0.94 | 0.00 | 3.15 | 0.00 |
| 5.0% | 20 | 1000 | 14.83 | 80.10 | 20.07 | 0.93 | 0.00 | 31.48 | 0.00 |
| 1.0% | 20 | 1000 | 2.98 | 16.02 | 4.02 | 0.93 | 0.00 | 6.30 | 0.00 |
| 0.5% | 20 | 1000 | 1.51 | 8.01 | 2.01 | 0.93 | 0.00 | 3.15 | 0.00 |

| Table B-3 Linear Variation in the x Direction T = -10 K alpha = $23.4 \times 10^{-6}$ | | | | | | | | | |
|---|---|---|---|---|---|---|---|---|---|
| Px | D/T | Rho | RMS | Span | Tilt | Focus | Astig | Coma | Sph Ab |
| 5.0% | 6 | Flat | 1.44 | 6.16 | 2.88 | 0.02 | 0.00 | 0.32 | 0.00 |
| 1.0% | 6 | Flat | 0.29 | 1.23 | 0.58 | 0.02 | 0.00 | 0.06 | 0.00 |
| 0.5% | 6 | Flat | 0.15 | 0.62 | 0.29 | 0.02 | 0.00 | 0.03 | 0.00 |
| 5.0% | 20 | Flat | 0.38 | 1.85 | 0.72 | 0.02 | 0.00 | 0.32 | 0.00 |
| 1.0% | 20 | Flat | 0.03 | 0.37 | 0.14 | 0.02 | 0.00 | 0.06 | 0.00 |
| 0.5% | 20 | Flat | 0.04 | 0.18 | 0.07 | 0.02 | 0.00 | 0.03 | 0.00 |
| 5.0% | 6 | 1000 | 147.55 | 798.79 | 198.55 | 9.40 | 0.00 | 314.82 | 0.01 |
| 1.0% | 6 | 1000 | 29.63 | 159.76 | 39.71 | 9.40 | 0.00 | 62.96 | 0.01 |
| 0.5% | 6 | 1000 | 15.00 | 79.88 | 19.86 | 9.40 | 0.00 | 31.48 | 0.01 |
| 5.0% | 20 | 1000 | 148.29 | 800.97 | 200.73 | 9.29 | 0.00 | 314.82 | 0.01 |
| 1.0% | 20 | 1000 | 29.77 | 160.19 | 40.15 | 9.29 | 0.00 | 62.96 | 0.01 |
| 0.5% | 20 | 1000 | 15.07 | 80.10 | 20.07 | 9.29 | 0.00 | 31.48 | 0.01 |

Table B-4 Linear Variation in the x Direction T = -10 K alpha = $23.4 \times 10^{-6}$

| Px | D/T | Rho | RMS | Span | Tilt | Focus | Astig | Coma | Sph Ab |
|---|---|---|---|---|---|---|---|---|---|
| 5.0% | 10 | Flat | 0.83 | 3.70 | 1.65 | 0.02 | 0.00 | 0.32 | 0.00 |
| 0.5% | 10 | Flat | 0.08 | 0.37 | 0.17 | 0.02 | 0.00 | 0.03 | 0.00 |
| 5.0% | 10 | 1000 | 147.97 | 800.04 | 199.80 | 9.34 | 0.00 | 314.82 | 0.01 |
| 0.5% | 10 | 1000 | 15.04 | 80.00 | 19.98 | 9.34 | 0.00 | 31.48 | 0.01 |
| 5.0% | 10 | 2000 | 73.67 | 399.10 | 98.98 | 4.65 | 0.00 | 157.41 | 0.00 |
| 0.5% | 10 | 2000 | 7.49 | 39.91 | 9.90 | 4.65 | 0.00 | 15.74 | 0.00 |
| 5.0% | 6 | 2000 | 73.26 | 397.86 | 97.73 | 4.66 | 0.00 | 157.41 | 0.00 |
| 0.5% | 6 | 2000 | 7.45 | 39.79 | 9.77 | 4.66 | 0.00 | 15.74 | 0.00 |
| 5.0% | 20 | 2000 | 73.99 | 400.02 | 99.90 | 4.63 | 0.00 | 157.41 | 0.00 |
| 0.5% | 20 | 2000 | 7.52 | 40.00 | 9.99 | 4.63 | 0.00 | 15.74 | 0.00 |
| 5.0% | 6 | 1000 | 147.55 | 798.79 | 198.55 | -9.40 | 0.00 | 314.82 | -0.01 |

Table B-5 Linear Variation in the x Direction T = -223 K alpha = $19.8 \times 10^{-6}$

| Px | D/T | Rho | RMS | Span | Tilt | Focus | Astig | Coma | Sph Ab |
|---|---|---|---|---|---|---|---|---|---|
| 5.0% | 6 | Flat | 27.25 | 116.25 | 54.32 | 0.35 | 0.00 | 5.95 | 0.00 |
| 1.0% | 6 | Flat | 5.45 | 23.25 | 10.86 | 0.35 | 0.00 | 1.19 | 0.00 |
| 0.5% | 6 | Flat | 2.73 | 11.63 | 5.43 | 0.35 | 0.00 | 0.60 | 0.00 |
| 5.0% | 20 | Flat | 7.12 | 34.87 | 13.63 | 0.35 | 0.00 | 5.95 | 0.00 |
| 1.0% | 20 | Flat | 1.43 | 6.97 | 2.73 | 0.35 | 0.00 | 1.19 | 0.00 |
| 0.5% | 20 | Flat | 0.72 | 3.49 | 1.36 | 0.35 | 0.00 | 0.55 | 0.00 |
| 5.0% | 6 | 1000 | 2784.14 | 15072.00 | 3746.47 | 177.40 | 0.00 | 5940.41 | 0.11 |
| 1.0% | 6 | 1000 | 559.11 | 3014.51 | 749.29 | 177.40 | 0.00 | 1188.08 | 0.11 |
| 0.5% | 6 | 1000 | 283.09 | 1507.26 | 374.65 | 177.40 | 0.00 | 594.04 | 0.11 |
| 5.0% | 20 | 1000 | 2798.02 | 15113.68 | 3787.60 | 175.36 | 0.00 | 5940.41 | 0.11 |
| 1.0% | 20 | 1000 | 561.82 | 3022.74 | 757.52 | 175.36 | 0.00 | 1188.09 | 0.11 |
| 0.5% | 20 | 1000 | 284.35 | 1511.37 | 378.76 | 175.36 | 0.00 | 594.04 | 0.11 |

Table B-6 Linear Variation in the z Direction T = -10 K alpha = $23.4 \times 10^{-6}$

| Pz | D/T | Rho | RMS | Span | Tilt | Focus | Astig | Coma | Sph Ab |
|---|---|---|---|---|---|---|---|---|---|
| 5.0% | 6 | Flat | 8.05 | 27.74 | 0.00 | 27.74 | 0.00 | 0.00 | 0.00 |
| 1.0% | 6 | Flat | 1.61 | 5.56 | 0.00 | 5.56 | 0.00 | 0.00 | 0.00 |
| 0.5% | 6 | Flat | 0.81 | 2.79 | 0.00 | 2.79 | 0.00 | 0.00 | 0.00 |
| 5.0% | 20 | Flat | 28.82 | 92.44 | 0.00 | 92.44 | 0.00 | 0.00 | 0.00 |
| 1.0% | 20 | Flat | 5.37 | 18.50 | 0.00 | 18.50 | 0.00 | 0.00 | 0.00 |
| 0.5% | 20 | Flat | 2.69 | 9.26 | 0.00 | 9.26 | 0.00 | 0.00 | 0.00 |
| 5.0% | 6 | 1000 | 10.92 | 37.63 | 0.00 | 37.63 | 0.00 | 0.00 | 0.02 |
| 1.0% | 6 | 1000 | 4.37 | 15.05 | 0.00 | 15.05 | 0.00 | 0.00 | 0.01 |
| 0.5% | 6 | 1000 | 3.55 | 12.22 | 0.00 | 12.22 | 0.00 | 0.00 | 0.01 |
| 5.0% | 20 | 1000 | 29.68 | 102.28 | 0.00 | 102.28 | 0.00 | 0.00 | 0.06 |
| 1.0% | 20 | 1000 | 8.08 | 27.89 | 0.00 | 27.89 | 0.00 | 0.00 | 0.02 |
| 0.5% | 20 | 1000 | 5.39 | 18.59 | 0.00 | 18.59 | 0.00 | 0.00 | 0.01 |

| Table B-7 Linear Variation in the z Direction T = -223 K alpha = $19.8 \times 10^{-6}$ | | | | | | | | | |
|---|---|---|---|---|---|---|---|---|---|
| Pz | D/T | Rho | RMS | Span | Tilt | Focus | Astig | Coma | Sph Ab |
| 5.0% | 6 | Flat | 151.90 | 523.51 | 0.00 | 523.51 | 0.00 | 0.00 | -0.00 |
| 1.0% | 6 | Flat | 30.46 | 104.98 | 0.00 | 104.98 | 0.00 | 0.00 | 0.00 |
| 0.5% | 6 | Flat | 15.28 | 52.67 | 0.00 | 52.67 | 0.00 | 0.00 | -0.00 |
| 5.0% | 20 | Flat | 506.05 | 1744.17 | 0.00 | 1744.17 | 0.00 | 0.00 | -0.00 |
| 1.0% | 20 | Flat | 101.29 | 349.11 | 0.00 | 349.11 | 0.00 | 0.00 | 0.00 |
| 0.5% | 20 | Flat | 50.70 | 174.73 | 0.00 | 174.73 | 0.00 | 0.00 | 0.00 |
| 5.0% | 6 | 1000 | 205.99 | 709.95 | 0.00 | 709.96 | 0.00 | 0.00 | 0.44 |
| 1.0% | 6 | 1000 | 82.37 | 283.91 | 0.00 | 283.91 | 0.00 | 0.00 | 0.18 |
| 0.5% | 6 | 1000 | 66.92 | 115.24 | 0.00 | 115.24 | 0.00 | 0.00 | 0.14 |
| 5.0% | 20 | 1000 | 559.96 | 1929.97 | 0.00 | 1929.98 | 0.00 | 0.00 | 1.20 |
| 1.0% | 20 | 1000 | 152.69 | 526.28 | 0.00 | 526.28 | 0.00 | 0.00 | 0.33 |
| 0.5% | 20 | 1000 | 101.79 | 350.82 | 0.00 | 350.82 | 0.00 | 0.00 | 0.22 |

Table B-8 Quadratic Variation in the z Direction T = -1 K alpha = $23.4 \times 10^{-6}$

| Pq | D/T | Rho | RMS | Span | Tilt | Focus | Astig | Coma | Sph Ab |
|---|---|---|---|---|---|---|---|---|---|
| 5.0% | 6 | Flat | 0.81 | 2.77 | 0.00 | 2.77 | 0.00 | 0.00 | 0.00 |
| 1.0% | 6 | Flat | 0.16 | 0.56 | 0.00 | 0.56 | 0.00 | 0.00 | 0.00 |
| 0.5% | 6 | Flat | 0.08 | 0.28 | 0.00 | 0.28 | 0.00 | 0.00 | 0.00 |
| 5.0% | 20 | Flat | 0.27 | 0.93 | 0.00 | 0.93 | 0.00 | 0.00 | 0.00 |
| 1.0% | 20 | Flat | 0.54 | 1.85 | 0.00 | 1.85 | 0.00 | 0.00 | 0.00 |
| 0.5% | 20 | Flat | 0.27 | 0.93 | 0.00 | 0.93 | 0.00 | 0.00 | 0.00 |
| 5.0% | 6 | 1000 | 1.09 | 3.77 | 0.00 | 3.77 | 0.00 | 0.01 | 0.00 |
| 1.0% | 6 | 1000 | 0.44 | 1.51 | 0.00 | 1.51 | 0.00 | 0.00 | 0.00 |
| 0.5% | 6 | 1000 | 0.36 | 1.22 | 0.00 | 1.22 | 0.00 | 0.00 | 0.00 |
| 5.0% | 20 | 1000 | 2.97 | 10.25 | 0.00 | 10.25 | 0.00 | 0.03 | 0.00 |
| 1.0% | 20 | 1000 | 0.81 | 2.79 | 0.00 | 2.79 | 0.00 | 0.01 | 0.00 |
| 0.5% | 20 | 1000 | 0.54 | 1.86 | 0.00 | 1.86 | 0.00 | 0.00 | 0.00 |

Table B-9 Quadratic Variation in the z Direction T = -10 K alpha = $23.4 \times 10^{-6}$

| Pq | D/T | rho | RMS | Span | Tilt | Focus | Astig | Coma | Sph Ab |
|---|---|---|---|---|---|---|---|---|---|
| 5.0% | 6 | Flat | 8.05 | 27.74 | 0.00 | 27.74 | 0.00 | 0.00 | 0.00 |
| 1.0% | 6 | Flat | 1.61 | 5.56 | 0.00 | 5.56 | 0.00 | 0.00 | 0.00 |
| 0.5% | 6 | Flat | 0.81 | 2.79 | 0.00 | 2.79 | 0.00 | 0.00 | 0.00 |
| 5.0% | 20 | Flat | 26.82 | 92.44 | 0.00 | 92.44 | 0.00 | 0.00 | 0.00 |
| 1.0% | 20 | Flat | 5.37 | 18.50 | 0.00 | 18.50 | 0.00 | 0.00 | 0.00 |
| 0.5% | 20 | Flat | 2.69 | 9.26 | 0.00 | 9.26 | 0.00 | 0.00 | 0.00 |
| 5.0% | 6 | 1000 | 10.93 | 37.68 | 0.00 | 37.68 | 0.00 | 0.00 | 0.08 |
| 1.0% | 6 | 1000 | 4.37 | 15.06 | 0.00 | 15.06 | 0.00 | 0.00 | 0.02 |
| 0.5% | 6 | 1000 | 3.55 | 12.23 | 0.00 | 12.23 | 0.00 | 0.00 | 0.01 |
| 5.0% | 20 | 1000 | 29.74 | 102.50 | 0.00 | 102.50 | 0.00 | 0.00 | 0.31 |
| 1.0% | 20 | 1000 | 8.11 | 27.94 | 0.00 | 27.94 | 0.00 | 0.00 | 0.07 |
| 0.5% | 20 | 1000 | 5.40 | 18.61 | 0.00 | 18.61 | 0.00 | 0.00 | 0.04 |

| Table B-10 Linear Variation in the r Dirction T = -10 K alpha = $23.4 \times 10^{-6}$ | | | | | | | | | |
|---|---|---|---|---|---|---|---|---|---|
| Pr | D/T | Rho | RMS | Span | Tilt | Focus | Astig | Coma | Sph Ab |
| 5.0% | 6 | Flat | 0.95 | 3.99 | 0.00 | -3.18 | 0.00 | 0.00 | 2.28 |
| 1.0% | 6 | Flat | 0.19 | 0.78 | 0.00 | -0.62 | 0.00 | 0.00 | 0.46 |
| 0.5% | 6 | Flat | 0.09 | 0.38 | 0.00 | -3.02 | 0.00 | 0.00 | 0.23 |
| 5.0% | 20 | Flat | 0.28 | 1.18 | 0.00 | -9.42 | 0.00 | 0.00 | 0.68 |
| 1.0% | 20 | Flat | 0.05 | 0.22 | 0.00 | -0.17 | 0.00 | 0.00 | 0.14 |
| 0.5% | 20 | Flat | 0.02 | 0.10 | 0.00 | -0.08 | 0.00 | 0.00 | 0.07 |
| 5.0% | 6 | 1000 | 1.84 | 5.92 | 0.00 | 6.31 | 0.00 | 0.00 | 2.17 |
| 1.0% | 6 | 1000 | 2.55 | 8.62 | 0.00 | 8.78 | 0.00 | 0.00 | 0.44 |
| 0.5% | 6 | 1000 | 2.64 | 9.01 | 0.00 | 9.09 | 0.00 | 0.00 | 0.22 |
| 5.0% | 20 | 1000 | 2.45 | 8.20 | 0.00 | 8.44 | 0.00 | 0.00 | 0.58 |
| 1.0% | 20 | 1000 | 2.65 | 9.08 | 0.00 | 9.12 | 0.00 | 0.00 | 0.12 |
| 0.5% | 20 | 1000 | 2.67 | 4.61 | 0.00 | 9.21 | 0.00 | 0.00 | 0.06 |

Table B-11 Linear Variation in the r Direction T = -223 K alpha = $19.8 \times 10^{-6}$

| Pr | D/T | Rho | RMS | Span | Tilt | Focus | Astig | Coma | Sph Ab |
|---|---|---|---|---|---|---|---|---|---|
| 5.0% | 6 | Flat | 17.82 | 75.21 | 0.00 | -60.07 | 0.00 | 0.00 | 42.98 |
| 1.0% | 6 | Flat | 3.49 | 14.76 | 0.00 | -11.74 | 0.00 | 0.00 | 8.59 |
| 0.5% | 6 | Flat | 1.69 | 7.21 | 0.00 | -5.69 | 0.00 | 0.00 | 4.30 |
| 5.0% | 20 | Flat | 5.28 | 22.31 | 0.00 | -17.77 | 0.00 | 0.00 | 12.90 |
| 1.0% | 20 | Flat | 0.98 | 4.18 | 0.00 | -3.28 | 0.00 | 0.00 | 2.58 |
| 0.5% | 20 | Flat | 0.44 | 1.92 | 0.00 | -1.46 | 0.00 | 0.00 | 1.29 |
| 5.0% | 6 | 1000 | 34.72 | 111.69 | 0.00 | 119.02 | 0.00 | 0.00 | 41.01 |
| 1.0% | 6 | 1000 | 48.09 | 162.72 | 0.00 | 165.72 | 0.00 | 0.00 | 8.29 |
| 0.5% | 6 | 1000 | 49.78 | 170.06 | 0.00 | 171.56 | 0.00 | 0.00 | 4.20 |
| 5.0% | 20 | 1000 | 46.20 | 154.77 | 0.00 | 159.19 | 0.00 | 0.00 | 10.88 |
| 1.0% | 20 | 1000 | 49.94 | 171.24 | 0.00 | 172.13 | 0.00 | 0.00 | 2.27 |
| 0.5% | 20 | 1000 | 50.41 | 173.30 | 0.00 | 173.74 | 0.00 | 0.00 | 1.19 |

# REFERENCES

1. S. Timoshenko and J. Goodier, Theory of Elasticity (New York: McGraw-Hill, 1970).